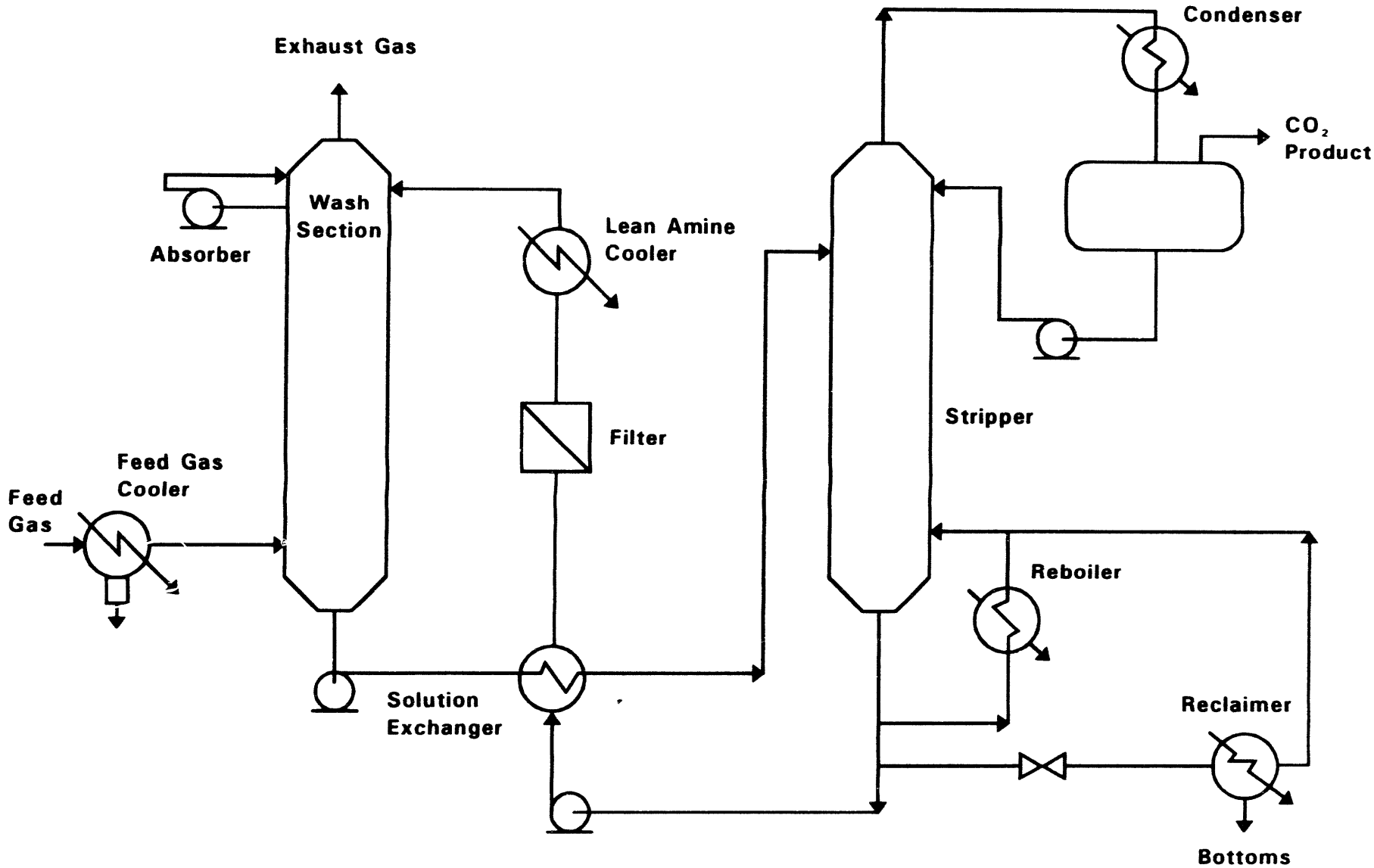

Figure 1. Kerr McGee/ABB Lummus Crest CO_2 Recovery Technology Basic Flow Scheme

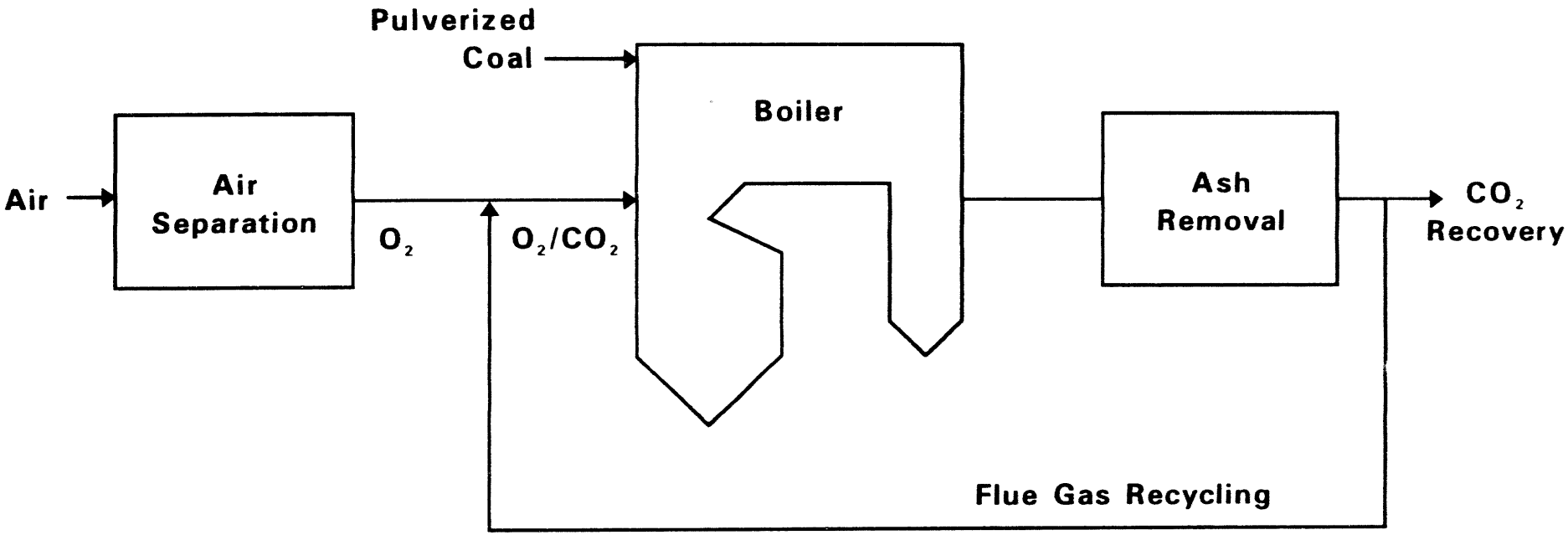

Figure 2. O_2/CO_2 Combustion Process

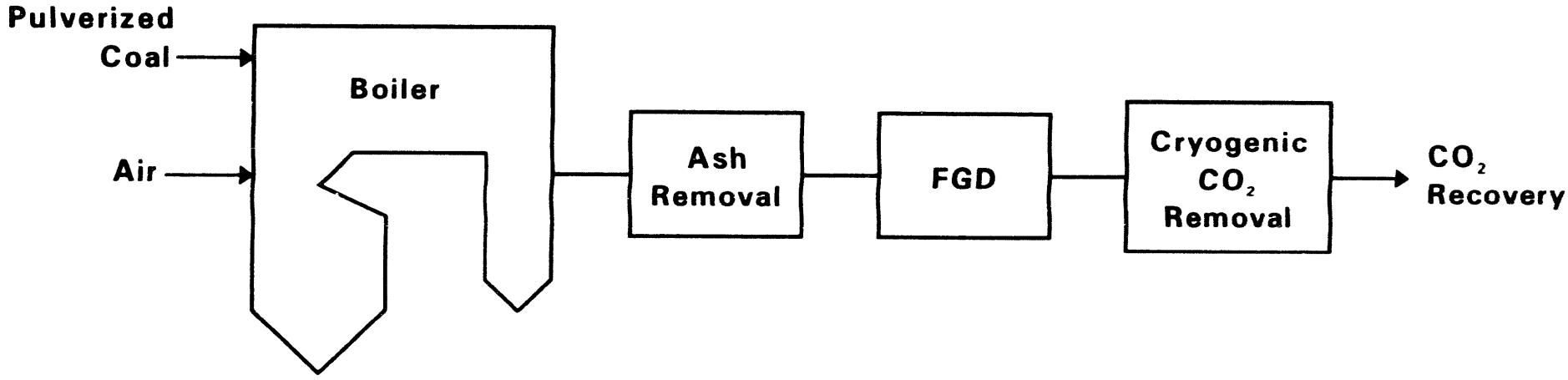

Figure 3. Cryogenic CO_2 Removal from Conventional PCF Power Plant

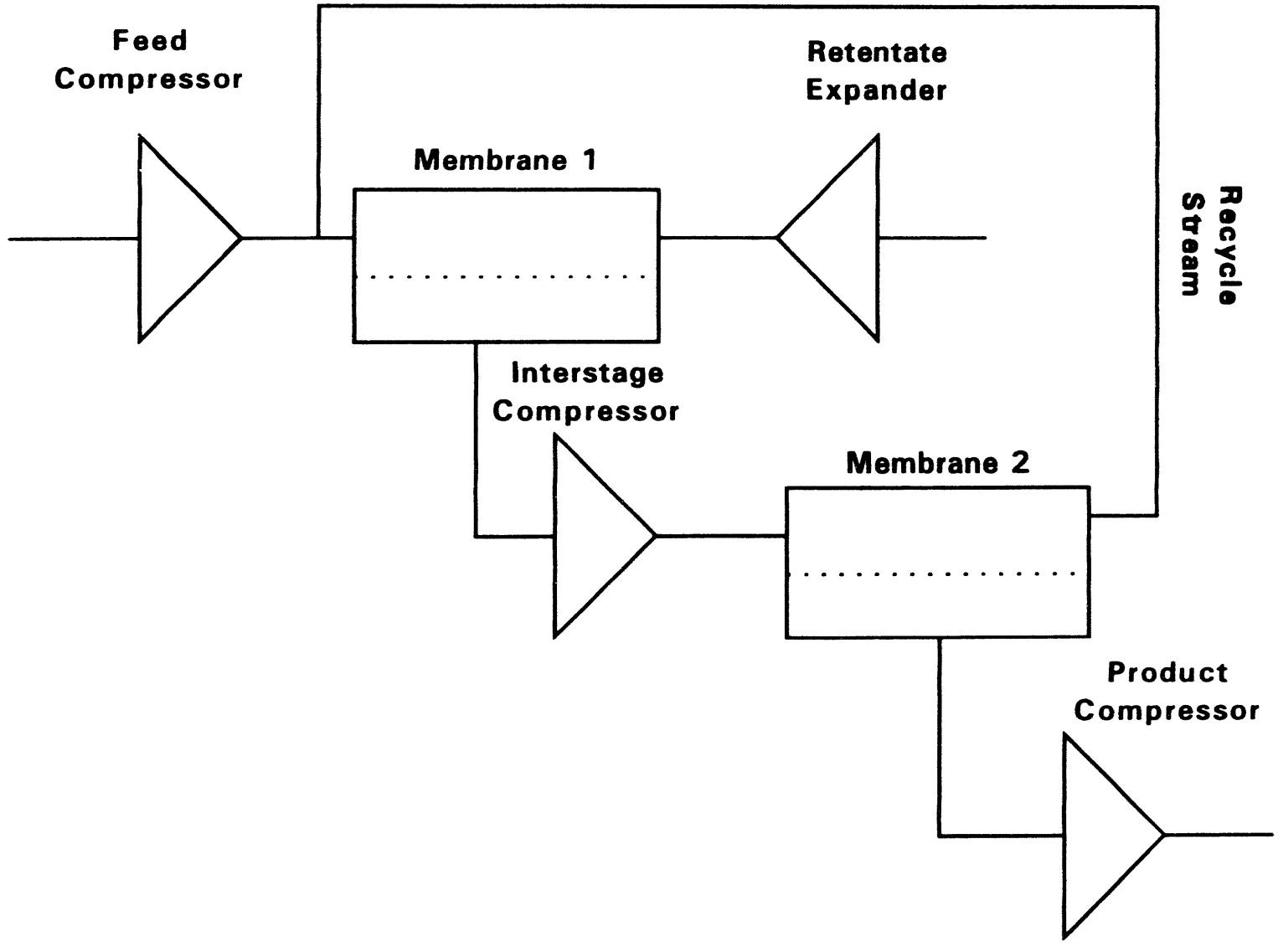

Figure 4. Lay Out of a Two Stage Cascade System

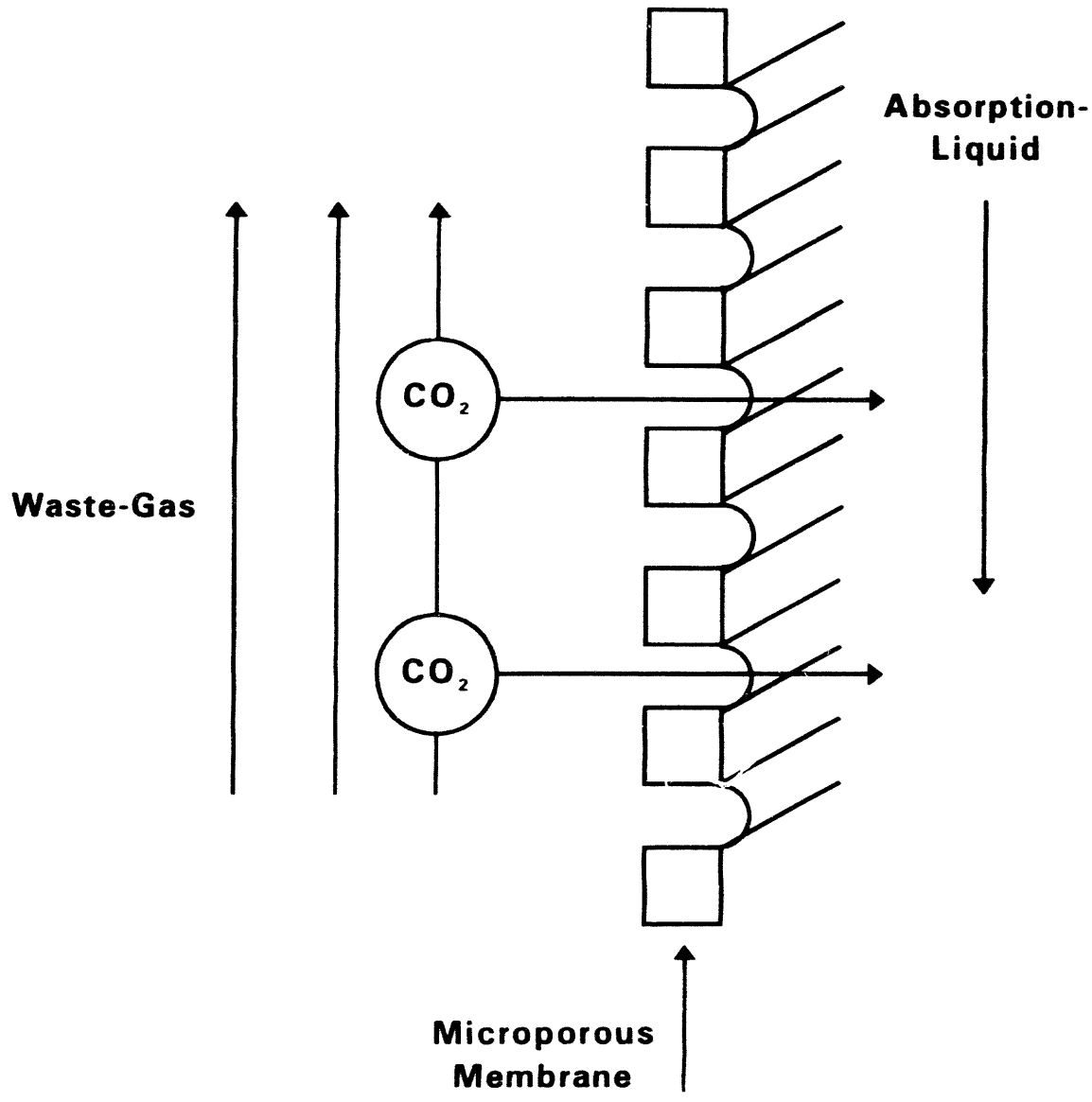

Figure 5. Gas Absorption Membrane Schematic

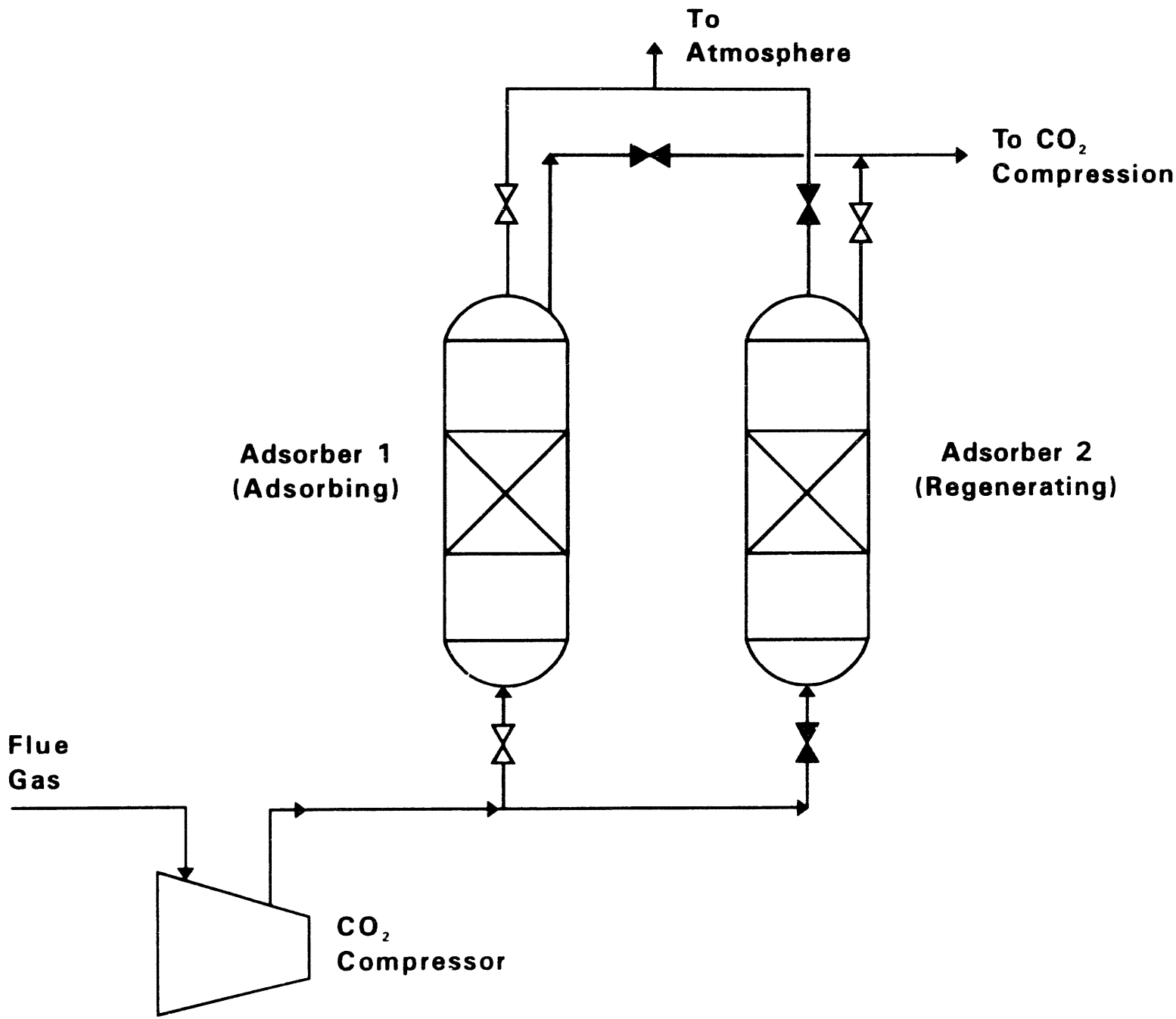

Figure 6. Pressure Swing Adsorption

The Carnol Process For Methanol Production and Utilization With Reduced CO_2 Emissions

Meyer Steinberg
Brookhaven National Laboratory
Upton, NY 11973

ABSTRACT

A first order comparative mass and energy analysis is made of alternative processes for the production and utilization of methanol. Conventional reforming of natural gas with steam and CO_2 indicates a yield of approximately 1 mol of methanol per mol of methane and a net emission of 1 mol of CO_2 per mol of methanol. Three new processes called Carnol I, Carnol II and Carnol III utilize CO_2 as a feedstock in conjunction with hydrogen produced from the thermal decomposition of methane can reduce CO_2 emission compared to the conventional process by 35%, 88%, and 100% respectively while reducing methanol production by 11%, 35%, and 39% respectively. The carbon from methane decomposition can be sequestered or sold as a commodity. The methanol can be used in the transportation sector as an alternative efficient fuel. A preliminary economic estimate indicates the equivalent cost for reduction of CO_2 to be less than estimates for removal, recovery, and disposal of CO_2 from power plant stack gas. The Carnol process leverages the CO_2 reduction both from central fossil fuel fired power plants and the transportation sector. The Carnol process assists in the reduction of CO_2 emission from an otherwise impossible collection of CO_2 from highly dispersed heat engine and small scale fuel users.

INTRODUCTION

Methanol is an environmentally preferred alternative transportation fuel and also can serve as a clean stationary power plant fuel. It can be produced from a number of carbonaceous feedstocks including natural gas, oil, coal, biomass (wood), and other agricultural products as well as municipal solid waste (MSW). Because of its abundance, relatively low cost, and processability, the preferred feedstock currently is natural gas (methane). There is also presently great interest in the direct utilization of CO_2 for purposes of reducing CO_2 emissions in order to mitigate the global greenhouse warming problem. One possibility is the utilization of large quantities of CO_2 for the production of such a potentially large scale fuel and chemical commodity as methanol. The following first reviews the conventional methods of reforming natural gas in Parts I, II, and III, and then the new Carnol processes are developed in Parts IV, V, and VI.

I. Conventional Method for Methanol Production with Steam Reforming

The conventional method for methanol production essentially consists of the steam reforming of natural gas to form carbon monoxide and hydrogen synthesis gas.[1] The synthesis gas is then sent to a methanol catalytic synthesis reactor for conversion to methanol. The excess hydrogen can be used in the reformer to provide the endothermic heat of the reforming operation. The reaction sequence is as follows:

1. Steam reforming: $H_2O + CH_4 = CO + 3H_2$
2. Methanol Synthesis: $CO + 2H_2 = CH_3OH$

Overall reaction: $H_2O + CH_4 = CH_3OH + H_2$

A mass and energy balance is made using standard thermodynamic functions[2]. Methane is used to heat the reformer. A summary of the results are listed in Table 1 under Column I and includes the CO_2 emissions per unit methanol produced.

II. Methanol with CO_2 Reforming

The conventional method of reforming methane with steam can also be conducted instead with CO_2. The resulting synthesis gas can be shifted and the CO and H_2 can then be converted to methanol. Methane combustion is used to provide the energy in the reformer. The reaction sequence is represented by the following set of reactions:

1.	Reforming:	$CO_2 + CH_4 = 2CO + 2H_2$
2.	Shift:	$0.67\ CO + 0.67\ H_2O = 0.67\ CO_2 + 0.67\ H_2$
3.	Removal and recovery of	CO_2 from coal fired power plant $= -0.67\ CO_2$
4.	Methanol Synthesis:	$1.33\ CO + 2.67\ H_2 = 1.33\ CH_3OH$
	Overall Net Reaction:	$0.33\ CO_2 + 0.67\ H_2O + CH_4 = 1.33\ CH_3OH$

A summary of the energy and mass balance is shown in Column II of Table 1.

III. Methanol with Steam and CO_2 Reforming

Reforming of CH_4 can take place both with steam and with CO_2 to produce a 2:1 mixture of H_2 and CO which is required for methanol synthesis. Methane combustion is used to supply heat to the reformer. The reactions in the reformer are as follows:

$$CH_4 + H_2O = CO + 3H_2$$

and $$0.5\ CH4 + 0.5\ CO_2 = CO + H_2$$

1.	Total Reforming:	$1.5\ CH_4 + H_2O + 0.5\ CO_2 = 2CO + 4H_2$
2.	Methanol Synthesis:	$4H_2 + 2CO = 2CH_3OH$
	Overall Net Reaction	$1.5\ CH_4 + 0.5\ CO_2 + H_2O = 2CH_3OH$

A summary of the calculated data is shown in Column III of Table 1.

IV. The CARNOL I Process for Methanol Synthesis for Reducing CO_2 Emission

There is, however, another method of utilizing CO_2 and CH_4 for the production of methanol which could reduce CO_2 emissions significantly but with a small reduction in methanol production per unit of methane. This process involves the gasification of carbon with CO_2 to produce CO and the production of carbon and hydrogen by the thermal decomposition of methane. Half of the carbon is then sequestered or sold and not burned and half is used in the gasification with CO_2. Finally, the CO from the gasification reaction is combined with the hydrogen from the decomposition of methane reaction to form methanol. Combustion of methane is used to heat the gasifier. The reaction sequence is as follows:

1.	Gasification:	$0.5\ CO_2 + 0.5C = CO$
2.	Methane Decomposition:	$CH_4 = C + 2H_2$
3.	Remove and sequester: or sell as Carbon:	$-0.5C$
4.	Methanol Synthesis:	$CO + 2H_2 = CH_3OH$
	Overall Net Reaction	$0.5CO_2 + CH_4 = 0.5C + CH_3OH$

A summary of the energy and mass requirements and net CO_2 emissions are shown in Table 1 under Column IV.

IV-A. Alternate Carnol IA Process for Methanol Synthesis

An alternate Carnol I process is also possible which yields very similar results to the above Carnol I process, deals with the reforming of methane with CO_2 instead of the gasification with CO_2 of part of the carbon from methane decomposition. Combustion of methane is used to drive the reformer. The reaction sequence then is as follows:

1.	Thermal decomposition:	$0.5\ CH_4 = 0.5\ C + H_2$
2.	Remove, store, or sell carbon:	$-0.5C$
3.	Reform methane with CO_2:	$0.5CH_4 + 0.5CO_2 = CO + H_2$
4.	Methanol synthesis:	$CO + 2\ H_2 = CH_3OH$
	Overall net reaction	$1CH_4 + 0.5CO_2 = 0.5C + CH_3OH$

A summary of the data for this system is also listed under Column IV in Table 1. Both Carnol Systems I and IA give the same results and are, therefore listed together in Table 1.

V. Carnol II Process for Methanol Synthesis for Reducing CO_2 Emission

A more efficient process for CO_2 emission reduction and production of methanol is devised as follows. Methane is first decomposed to carbon and hydrogen. The carbon is not burned; it can be stored or sold as a commodity like carbon black. The hydrogen is then reacted with CO_2 to form methanol. The CO_2 can come from scrubbing and recovery of CO_2 from power plant stacks, wells, and ammonia plants. Methane is used to provide the endothermic energy for the thermal decomposition of methane for hydrogen production.

The reaction sequence is as follows:

1.	Methane Decomposition	$3CH_4 = 3C + 6H_2$
2.	Methanol Synthesis	$2CO_2 + 6H_2 = 2CH_3OH + 2H_2O$
	The overall net reaction	$3CH_4 + 2CO_2 = 2CH_3OH + 2H_2O + 3C$

It should be noted that the methanol synthesis from CO_2 and $3H_2$ instead of the conventional CO and $2H_2$ is not unusual. There are catalysts available to accomplish this and indeed there are several commercial plants operating with CO_2 currently[1]. A summary of the mass and energy balances for Carnol II are given in Col. V in Table 1.

VI. Carnol III Process for Methanol Synthesis for Zero CO_2 Emission

A final version of the Carnol process which results in zero CO_2 emission is designed as follows. Methane is decomposed to carbon and hydrogen. Part of the hydrogen is used to provide the endothermic energy for decomposition of methane. Thus, there is no generation and emission of CO_2. The larger remaining part of the hydrogen is reacted with CO_2 from external sources to produce the methanol. The reaction sequence for Carnol III is the same as for Carnol II as follows:

1.	Methane decomposition	$3CH_4 = 3C + 6H_2$
2.	Methanol Synthesis	$2CO_2 + 6H_2 = 2CH_3OH + 2H_2O$
	Overall Net Reaction	$3CH_4 + 2CO_2 = 2CH_3OH + 2H_2O + 3C$

A summary of the data for this system is shown in Column IV in Table 1.
A schematic of Carnol III is shown in the inset of Figure 1.

COMPARATIVE ANALYSIS

A comparative analysis can now be made of the six systems described above and summarized in Table 1. Table 2 gives data comparisons for the methanol yields and CO_2 emission for the Carnol processes. The three conventional reforming systems: (I) steam, (II) CO_2, and, (III) steam and CO_2 reforming, yield approximately 1 mol methanol produced per mol of methane consumed and each emits a net of approximately 1 mol CO_2 per mol of methanol produced and eventually consumed as fuel.

In the new CARNOL I or IA processes, when the methanol is used as fuel, the CO_2 emission can be reduced by 35% from that produced by the conventional reforming processes. This CO_2 reduction, however, is obtained with an 11% decrease in methanol production per unit of methane compared to the reforming processes. The CO_2 fixed for Carnol I is only 0.42 mol CO_2 per mole of CH_4 feedstock and the carbon yield is 0.5 mole per mol of methanol produced.

In the new CARNOL II process the CO_2 emission can be reduced by as much as 88%. However, this larger reduction is obtained at the expense of reducing methanol production per unit of natural gas by 35%, compared to the base conventional reforming system I. The amount of CO_2 feedstock for Carnol II is 0.61 moles CO_2 per mol CH_4 feedstock and the carbon yield is increased to 1.5 moles per mol of methanol produced.

In the new Carnol III process the CO_2 emission is completely eliminated. The penalty for achieving zero CO_2 emission is the reduction of methanol production per unit of natural gas by 39% compared to conventional reforming. The thermal efficiency of conversion of the methane to methanol is reduced to 50%. The amount of CO_2 fixed for Carnol III is 0.58 moles CO_2 per mole CH_4 feedstock and the carbon yield is increased to 1.73 moles C per mole of methanol product.

It should be pointed out that in this first order analysis the additional energy due to inefficiency of energy recovery in the reformer and decomposer combustors and the energy for compression is not accounted for in the above estimates. These energy requirements in terms of fuel methane relative to the methane requirement for the process gas are relatively small and should not alter the general comparative conclusions of this fundamental first order assessment.

ECONOMIC CONSIDERATIONS

A preliminary economic evaluation of the new Carnol III process in terms of the cost of eliminating CO_2 emission can be made based on the assumptions listed in Table 3.

The total methanol production cost and selling price for Carnol III is 0.59/gal MeOH which assumes $2.00 MSCF of natural gas and storing the carbon. Thus, Carnol III methanol costs $0.14/gal more than the current selling price of methanol at $0.45/gal. If the natural gas cost increases to $3.00/MSCF the production cost increases to $0.73/gallon and the incremental cost increases to $0.28/gal CH_3OH. At $2.00/MSCF CH_4 the incremental cost of the methanol translates to $18/ton CO_2 emission reduction. To put this cost of reducing CO_2 in perspective, the minimum estimated cost for CO_2 emission reduction by removal, recovery and disposal in depleted gas wells and the ocean, from stationary sources such as power plants is estimated to be in the range of $18 to $45/ton of CO_2[5,6]. Thus, at an average cost of CO_2 reduction of $32/ton CO_2 the above Carnol III CO_2 reduction cost of $18/ton CO_2 is 44% lower.

If a value can be placed on the carbon black to be sold as a marketable commodity not only can the cost of avoiding emission of CO_2 be reduced, but also a credit can be applied to the methanol cost to reduce its selling price. This is not unreasonable. For example, carbon black demands anywhere from $0.10/lb ($200/ton) to $0.50/lb

($1000/ton) depending on the use and grade. The large markets for carbon are for rubber tire vulcanization, pigments in paints and for, water purification. For Carnol III the carbon production per unit of methanol is 4.28 Lb. C/gal CH_3OH. If the carbon can be sold at $0.10/lb, then the income from the carbon = $0.10 x 4.28 = $0.43/gal CH_3OH. Applying this credit of carbon sales to the cost of Carnol III methanol, the selling price of methanol is reduced to $0.16/gal., which is 65% lower than the current selling price of $0.45/gal. By selling the carbon at $0.05/lb. (which is the fuel oil equivalent energy value at $20/bbl oil) then the income from carbon is 0.05 x 4.28 = $0.21/gal CH_3OH and the methanol can sell for $0.38/gal. Furthermore, if the efficiency of methanol claimed by EPA is 30% greater for methanol cars than for gasoline cars (i.e., 1.54 gallons methanol is equivalent to 1 gallon gasoline)[7], at a selling price of $0.45/gal the equivalent gasoline cost for methanol is $0.73/gal. The 1992 refined price for gasoline with oil at $20/bbl amounted to about $0.73/gal. The conclusion is that not only can Carnol III reduce CO_2 emission at an equivalent competitive price compared to other means of CO_2 avoidance, but can supply the transportation market at a price competitive with petroleum based fuel. Table 3 summarizes the above economic arguments for Carnol III.

It is interesting to note that a coal fired power plant can remove and recover CO_2 for supply to a Carnol III plant to produce methanol which in turn can be used in the transportation sector, as well as other dispersed smaller users of fuel. 1.6 mols of natural gas (CH_4) in the Carnol III plant removes one mol of CO_2 produced from 1 mol of coal ($CH_{0.8}$ $O_{0.1}$) from a coal fired power plant which is sequestered or sold as carbon. The methanol can then be used as a fuel in the automotive industry which gains another 39% reduction in CO_2 emissions. Furthermore, this is obtained from a highly dispersed source for which there is no other easy means of removal and recovery. Thus, natural gas with Carnol, leverages both the coal fired power plant and the automotive industry in obtaining a significant reduction in CO_2 emission. Figure 1 shows the sequence of this flow of feedstock and product streams.

An interesting question arises as to which sector should bear the cost of CO_2 reduction; the power plant, the methanol Carnol plant or the automotive methanol or smaller user? The answer to this question depends on whether there will be an environmental government regulation or taxation applied to CO_2 emissions from fossil fuel plants. If there is no regulation, then (1) the cost of CO_2 recovered from the power plant can be charged to the Carnol methanol plant, and (2) the carbon coproduct from the Carnol plant can be used or sold as fuel or as a material commodity. If regulation or taxation becomes an economic requirement imposed by government rule, the Carnol process application will come about more quickly and then, (1) the Carnol plant can actually charge the power plant disposal costs because the Carnol plant will provide a service for the power plant in getting rid of the CO_2, and (2) the carbon will either be sequestered or sold as a commodity but prohibited as a fuel. By the same token, the automotive industry should pay the Carnol plant for reducing the CO_2 emissions from vehicles by supplying more efficienct CO_2 reducing methanol.

One possible accounting can be made as follows and illustrated in Figure 1. As mentioned earlier, the CO_2 sequestering cost for the power plant is estimated to be $32/ton CO_2 and the cost of recovery of CO_2 is estimated to be $25/ton CO_2[6]. Therefore, the power plant can pay the Carnol plant up to the sequestering cost of $7/ton CO_2 or in terms of per unit of methanol (7/127) or $0.06/gal methanol. Since the total cost of methanol by the Carnol process with $2.00/MSCF methane is $0.59/gal in order to bring it to conventional methane cost of $0.45/gal, $0.14/gal must be made up. Since the power plant has paid $0.06 already, the automotive industry should pay the difference or $0.08/gal, which is only $10/ton of CO_2 avoided, which is fairly reasonable. Thus, the automotive industry will pay (0.45 + 0.08) or $0.53/gal or the

equivalent of $0.82/gal of gasoline which is 11% higher than the 1990 refining price of $0.73/gal, which is not too unreasonable. In the meantime, if the carbon can be sold for $0.05/lb then the credit to the Carnol plant amounts to $0.21/gal and an additional $0.03/gal is credited since sequestering is avoided and the net methanol cost is reduced (0.45-0.24) to $0.21/gal. Some of the savings can be returned to both the power plant and the automotive industry to reduce the cost. Furthermore, serious development work is progressing on the use of methanol in fuel cells in automobiles which is aimed at improving the efficiency of the use of methanol by more than a factor of 2 compared to present IC engines. This would significantly reduce CO_2 emissions and make the use of methanol much more economical.

An important final point can be made concerning the Carnol process, and that is, it avoids the disposal of CO_2 in the ocean, as well as the need for growing rapid rotational crop biomass in energy farms in order to capture CO_2. However, the addition of biomass can further reduce CO_2 emissions if it substitutes as an alternative fuel to fossil fuels in power plants.

Conclusion

The conclusion of this first order evaluation of alternative processes, appears to be that there is a decided benefit in pursuing the development of the CARNOL processes for purposes of utilizing CO_2 recovered from power plants and significantly reducing the net CO_2 emissions in the production and utilization of methanol as an alternative liquid fuel for the transportation fuel market, as well as, the stationary fuel user market.

References:

1. Faith, Keyes, Clarke, "Industrial Chemicals, 4th Edition John Corley and Sons, New York, (1975).

2. Thermodynamic values taken from JANAF Thermodynamic Tables, 2nd Edition, NSRD-NBS 37, National Bureau of Standards, Washington, DC (1971).

3. Chemical Week 153, NO. 4, p. 42 (August 4, 1993).

4. J. Korchnak, J. Brown Engineers, Inc., private communication, (1991).

5. W.C. Turkenburg, "CO_2 Removal, Some Conclusions", Proceedings of the First International Conference on Carbon Dioxide Removal p. 821, Pergamon Press, Oxford, U.K. (1992).

6. Greenhouse Issues, No. 7, IEA Greenhouse Gas R&D Programs, Chiltenham, U.K. (March 1993).

7. Office of Mobil Sources, "An Analysis of the Economic and Environmental Effects of Methanol as an Automotive Fuel," EPA Report No. 0730 (NTIS PB90-225806), Motor Vehicle Emissions Laboratory, Ann Arbor, MI, (1989).

TABLE 1
COMPARATIVE ANALYSIS FOR METHANOL PRODUCTION

PROCESS	I. CONV. STEAM REF.	II. CONV. CO_2 REF.	III. CONV. STEAM AND CO_2 REF.	IV. & IVA. CARNOL I & IA PROCESS	V. CARNOL II PROCESS	IV. CARNOL III PROCESS
Energy for process (Kcal/mol MeOH)	60	45	45	39	27	31
Yield MeOH MeOH/CH_4 (mol/mol)	0.95	1.04	1.01	0.85	0.62	0.58
CO_2 Emission (mol CO_2/ mol MeOH)	1.05	0.96	0.99	0.68	0.13	0.00
Gasifier Shift or Reformer Reactor	YES	YES	NO	YES	NO	NO
Acid gas removal	NO	YES	NO	NO	NO	NO
Carbon yield Mol C/Mol MeOH	0	0	0	0.5	1.5	1.73
No. of Reactors	2	4	2	3	2	2
Percent CO_2 reduction from base %	BASE	-9	-6	35	88	100

TABLE 2

CARNOL PROCESSES FOR METHANOL PRODUCTION
AND UTILIZATION
FOR REDUCING CO_2 EMISSION REDUCTION

FEEDSTOCK - NATURAL GAS CO_2 FROM POWER PLANT STACKS SEQUESTER OR SELL CARBON -		
PROCESS	% REL.* MeOH PRODUCTION	REL.* CO_2 EMISSION REDUCTION
CARNOL I OR IA C GASIF. OR CH_4 REFORMING	89%	35%
CARNOL II CH_4 FOR REFORMING AND COMBUSTION	65%	88%
CARNOL III H_2 COMBUSTION	61%	~100%

*REL. means relative to a conventional natural gas to methanol plant

TABLE 3
ECONOMICS OF CO_2 REDUCTION FROM THE
CARNOL III PROCESS
ZERO CO_2 EMISSION

Current Selling Price MeOH	=	$0.45/gal
Natural Gas Cost	=	$2.00/MSCF
CO_2 Cost from Power Plant	=	$0.00
Cost of Sequesting Carbon	=	$15/ton
Plant Factor	=	90% on line
Unit Capital Cost	=	$139,000/t day-methanol
Fixed Charges	=	21%
MeOH Production Cost at 3.0¢/MSCF NG	= =	$0.59/gal $0.73/gal
Cost of Reducing CO_2 based on Increased MeOH Cost	= =	$18/ton CO_2 (44% lower than $32/ton CO_2
Cost of Removal, Recover, & Disposal in Ocean Aquifer From PC Power Plants	=	$32/ton CO_2
Taking Credit for 38% Reduction CO_2 Emission in MeOH Fueled Vehicles - S.P. MeOH	=	$0.45/gal
If Carbon is sold, MeOH cost: with no MeOH vehicle credit: @ $0.10/Lb C Credit @ $0.05/Lb C Credit	 = =	 $0.16/gal $0.38/gal
Equivalent Cost of Gasoline (1.54 gal MeOH = 1 gal Gasoline)	=	$0.73/gal* (at $0.45/Gal Methanol)

$0.73/gal is current (1992) refining price of gasoline based on $20/bbl of oil.

Figure 1

CARNOL PROCESS FOR METHANOL PRODUCTION

TO REDUCE CO2 EMISSION FROM POWER PLANTS AND AUTOMOTIVE ENGINES

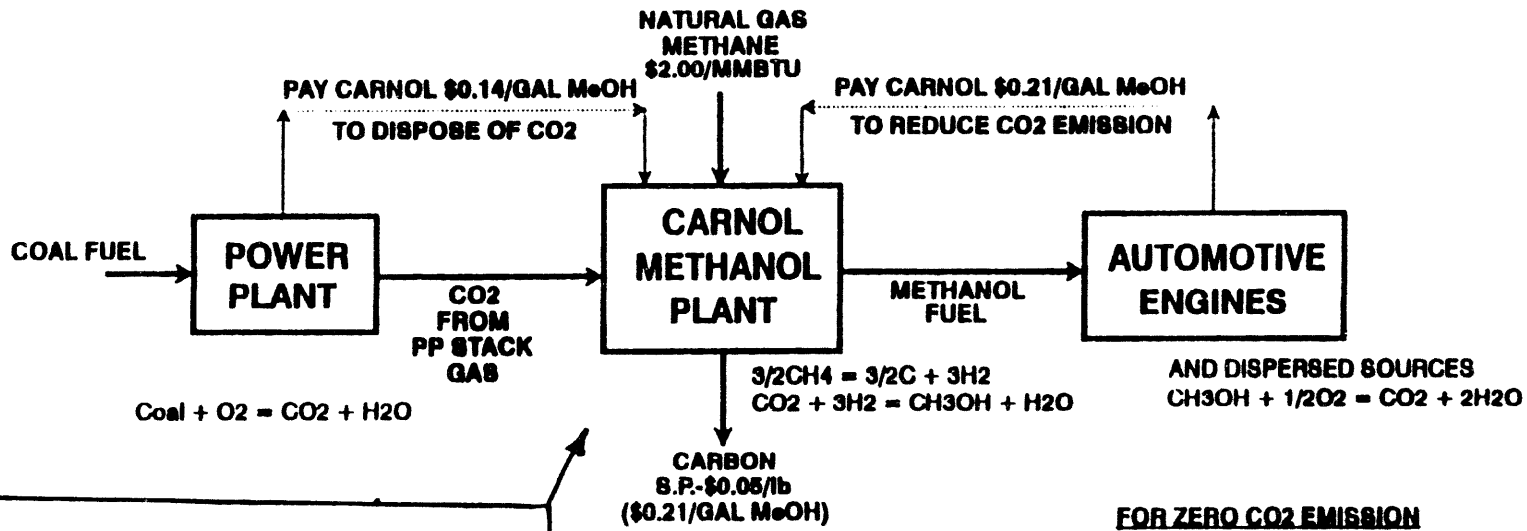

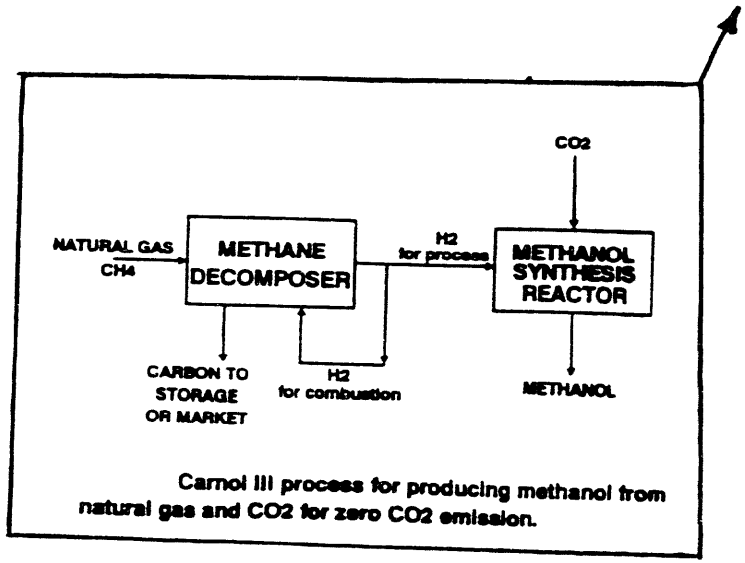

Carnol III process for producing methanol from natural gas and CO2 for zero CO2 emission.

SYSTEMS AND ECONOMIC ANALYSIS OF MICROALGAE PONDS FOR CONVERSION OF CO_2 TO BIOMASS

JOHN R. BENEMANN
DEPARTMENT OF CIVIL ENGINEERING
UNIVERSITY OF CALIFORNIA BERKELEY
BERKELEY, CA 94720

SUMMARY

Microalgae cultivation in large open ponds is the only photosynthetic process likely to directly utilize power plant flue gas CO_2 for production of biomass. The algal biomass can be converted into substitutes for fossil fuels, in particular liquid fuels such as biodiesel (vegetable oil methyl or ethyl esters), thus reducing atmospheric CO_2 levels and the potential for global warming. This concept is being investigated, among others, at the National Renewable Energy Laboratory at Golden Colorado, with support from PETC.

Microalgae biomass is currently being produced for food supplements in the U.S. at three commercial facilities, each about 10 hectare in size and producing several hundred tons of algae at a cost of over $10,000/ton. In scale, productivities and costs, microalgae biomass production technology must advance by an order of magnitude to be considered as an alternative fuel source and CO_2 mitigation technology.

Previous economic analyses of this concept, based on a number of favorable technical and site-specific assumptions, concluded that the large-scale (1,000 ha; 100,000 mt/y) production of microalgae could, in principle, be feasible technically. To be economically competitive with fossil fuels would require sites where low cost land and water are available and climatic conditions highly favorable. The prior studies had many limitations: mass balances and cost estimates were uncertain, designs not sufficiently detailed; the interface between the power plant stack gases and the microalgae production systems not addressed, and many of the scientific and engineering assumptions made were not sufficiently justified. For example, very high productivities were assumed, but how these were to be achieved was not detailed. Harvesting of the algae postulated a bioflocculation process, which remains to be demonstrated. Perhaps most important, the generic nature of those analysis did not consider constraints imposed by site specific factors.

Since these earlier feasibility studies, considerable experience has been gained in commercial microalgae production, and advances have been made in a number of fields related to this subject. An updated, more detailed and site specific, feasibility and economic analysis of microalgae systems for CO_2 capture from coal-fired power plants is being carried out under this project. A detailed review the prior work in this field has been completed, cost estimates for pond construction refined, and sites in California and Florida, are being selected for a site specific cost analysis. This project should allow an assessment of the potential of microalgae production as a process for CO_2 mitigation.

INTRODUCTION

Microalgae comprise a vast assemblage of organisms characterized both by their microbial nature and their ability to produce oxygen through photosynthesis. They generally are single cell organisms or undifferentiated filaments or colonies. They grow suspended in water (planktonic forms) or attached to surfaces. The microalgae include procaryotes (cyanobacteria or blue-green algae) and eucaryotes (green algae, red algae, diatoms, etc.). Between and even within the thousands of known species there is great metabolic and physiological diversity.

Microalgae production combines characteristics of plant photosynthesis and microbial fermentations: high growth rates and hydraulic production systems using light, CO_2, and inorganic nutrients. Microalgae production R&D was initiated forty years ago in the U.S., with human food production as a major goal (Burlew, 1953). Over the past four decades microalgae production has been investigated in many countries for this and many other applications: human and animal waste treatment, fuels production, heavy metal sequestration, atmosphere regeneration in space vehicles, fertilizers, xanthophlls (pigments useful in animal feeds), omega-3 fatty acids, amino acids and vitamins, diagnostic reagents, surfactants, industrial polysaccharides and other specialty chemicals, and, of particular interest recently, CO_2 utilization from power plants for greenhouse gas mitigation (Benemann, 1992).

A major practical application of algal pond culture has been in the field of wastewater treatment. However, in such ponds algal species are not controlled and the biomass is seldom harvested. The first large-scale (> 1 ton/month) commercial microalgae production, of the single cell green alga Chlorella, was established in Japan during the early 1960's. Chlorella is sold as food supplements ("health foods"), and most production is currently located in Taiwan.

Production of the filamentous blue-green alga Spirulina, a traditional food in several countries, was initiated in Mexico about 1974. It is now also being produced in several other countries, including the U.S. where two large (> 200 tons/year) production plants are operating in California and Hawaii. Spirulina is sold mainly as a food supplement, but is also used to extract a blue pigment, phycocyanin, used as a food coloring agent in Japan, and in specialty animal and aquaculture feeds.

The third microalga already being produced commercially is the green alga Dunaliella, which grows in hypersaline environments and contains high amounts of beta-carotene, a pro-vitamin A, food coloring agent, and a reputed anticancer agent. These currently produced microalgae are sold at prices exceeding $10,000/ton of organic dry weight. The production of microalgae for CO_2 utilization and fuels production requires production costs below $500/ton. This project addresses the question of whether it could be feasible to reduce costs by such a large factor.

AIR TOXICS & MERCURY MEASUREMENT AND CONTROL WORKSHOP

CURRENT COMMERCIAL MICROALGAE PRODUCTION

Current costs for commercial microalgae production are high for several reasons: small-scale of production, low productivities, high harvesting and processing costs and high capital costs. Chlorella cultivation systems become easily contaminated. Spirulina, a filamentous blue-green alga, requires a high (> 15 g/l) bicarbonate medium and Dunaliella requires high (> 100 g/l) NaCl concentrations, both of which add to production costs and reduce productivities, also provide a selective chemical environment that minimizes most contamination problems.

A fundamental issue is the design of the cultivation system, the "photobioreactor". Many designs have been proposed and tested, from small laboratory devices to open ponds many hectares in size. The design of such systems is constrained by the need to provide light (large surface to volume ratios), control environmental conditions (pH, temperature, dissolved oxygen, etc.), supply nutrients (mainly CO_2; also N, P, etc.), and control contamination (other algae, grazers, etc.). Of course, the ultimate constraint is economic, dictated by the value of the product.

The two main system designs are used in large-scale microalgae cultivation:

1. Shallow (< 30 cm), paddle wheel mixed, raceway pond design, which allows good control over conditions (such as CO_2 supply). Individual growth ponds are currently up to about 0.5 ha in size and are plastic lined, although much larger sizes and unlined ponds should be, at least theoretically, feasible.
2. Relatively deep (typically > 50 cm), large (> 1 ha, with some as large as 100 ha), unlined ponds, not mechanically mixed, relying mainly on wind mixing.

The latter design provides little possibility for process control, and is used in waste water treatment, by one plant in Mexico for Spirulina production, and by two plants for Dunaliella production systems in Australia. However, productivities are very low in such systems and they would not be practical for CO_2 utilization. Only the "raceway" design can achieve the high productivities required. Table 1 lists the three commercial raceway ponds production facilities in the U.S. Other commercial plants based on the same design are operating in Israel (for Dunaliella) and Thailand (for Spirulina).

Table 1. U.S. Commercial Microalgae Production Facilities

Alga	Location	Area (ha)	Production (t/y)
Spirulina	So. Calif.	8	200
Spirulina	Hawaii	6	200
Dunaliella	So. Calif.	5	< 50

MICROALGAE FUEL PRODUCTION AND CO_2 MITIGATION

The possibility of low-cost production of microalgae has attracted the attention of researchers for the past four decades starting with the work described in Burlew (1953). Oswald and Golueke (1960) first analyzed the possibility of growing microalgae on power plant flue gases (as a source of CO_2), and converting the biomass to methane gas, which could be used as a fuel to operate the power plant. This concept, of coupling algae production with power plant CO_2 utilization, and thus replacing fossil fuels, has received renewed attention with the concern about possible global warming due to CO_2 emissions.

The energy crisis of the 1970's had already spurred research on microalgae production for fuels. The U.S. Department of Energy, in large part through the Aquatic Species Program of the National Renewable Energy Laboratory (NREL, formerly SERI, the Solar Energy Research Institute), has sponsored almost $20 million in basic and applied microalgae production research, with the objective of developing low cost technology for microalgae fuel production (Neenan et al., 1986). The emphasis of this program is on the production of liquid fuels, specifically vegetable oils that can be rather readily converted to "biodiesel". Microalgae, under certain conditions (such as N limitation) produce copious amounts of oils, a phenomenon studied for over 50 years. A pilot plant facility located in Roswell, New Mexico, demonstrated the feasibility of cultivating various species of microalgae on saline ground waters (Weissman and Tillett, 1989, 1992). The use of water resources unsuitable for agriculture is a requirement for such a process. An ambitious program on using microalgae for CO_2 mitigation was recently established in Japan.

The goal of producing fuels with microalgae may seem improbable considering the relatively high present costs of producing microalgae, well over one order of magnitude higher than those allowable for fuel production and CO_2 utilization. However, several factors could greatly reduce the cost of microalgae production:

1. Increases in scale of operation, from the less than 10 ha scale of current facilities to about 1,000 ha for a fuel production/CO_2 utilization system;
2. The use of unlined earthwork ponds, rather than plastic lined ponds;
3. The ability to maintain a stable culture, overcoming grazer invasions and other biological invasions at essentially no cost or loss of productivity.
3. The use of cheaper harvesting methods, such as bioflocculation (the spontaneous flocculation and settling of algal cells, Benemann et al., 1980);
4. The development of low cost processing of algal biomass to fuels; and
5. Increasing the productivity of algal cultures, from currently under 50 mt/ha-yr for commercial systems to near the theoretical maximum of 200 mt/ha-yr.

Indeed, previous economic analysis carried out by the author and colleagues (Benemann et al., 1982; Weissman and Goebel, 1987) suggest that, in principle, very low cost production systems are feasible, as reviewed next.

PROJECTED COSTS FOR LARGE-SCALE MICROALGAE PRODUCTION

The cost estimates, summarized in Table 2, reflect numerous favorable assumptions about both the engineering and biological aspects of such a process. The individual growth ponds would be earthwork construction, unlined, paddle wheel mixed raceway designs, with a single central baffle and about 10 ha in size. Contamination or grazing problems are ignored. Harvesting would be by bioflocculation. Available water would contain sufficient alkalinity to allow CO_2 storage. Very high productivities are assumed, up to the theoretical limit. Although design of some of the subsystems are based on significant detail (e.g. paddle wheels), others (such as the interface of the power plant, the flue gas distribution system and the processing of the algal biomass to oil) are based on very superficial estimates. Very favorable site characteristics are assumed, in terms of climate, land slope, soil properties, and availability of land and water at essentially zero costs.

Table 2. Capital and Operating Costs for Microalgae Fuels
(Based on a 1,000 Ha algae production facility)

Productivity Assumed:	**Current**	**Maximum**
(ash-free dry weight)	**Projected**	**Theoretical**
Average Daily:	30 g/m^2-d	60 $g/m^2/d$
Annual:	109 mt/ha-yr	219 mt/ha/yr
Capital Costs ($/ha):		
Ponds (earthworks, CO_2 sumps, mixing)	27,500	33,000
Harvesting (settling ponds, centrifuges)	12,500	17,000
System-wide Costs (water, CO_2 supply, etc.)	30,000	40,000
Processing (oil extraction, digestion)	10,000	20,000
Engineering, Contingencies (25% of above)	20,000	27,500
Total Capital Costs ($/ha)	100,000	137,500
Capital Costs $/t-yr	920	630
Barrels of Oil/ha-yr (@ 3.5 bar./t)	380	760
Capital Costs $/Barrel-yr	260	180
Operating Costs ($/ha-yr):		
Power, nutrients, labor, overheads, etc.	10,000	15,500
Credit for methane produced	- 3,000	- 6,000
Net Operating Costs $/ha-yr	7,000	9,500
Net Operating Costs $/barrel oil	18	13
CO_2 Mitigation Credits ($60/tC)	-10	-10
Annualized Capital Costs (0.2 x Capital)	52	36
Total Costs $/Barrel	**60**	**39**
Land Area Required ha/MW:	**12**	**6**

Assumptions: Algae organic composition: 50% lipid, 25% carbohydrate, 25% protein, 60% C, 5% N, heat of Combustion: 7.5 Kcal/g.
Avg. Annual Solar Insolation: 500 Langleys, 45% visible.

LARGE-SCALE MICROALGAE PRODUCTION FOR FLUE-GAS CO_2 UTILIZATION

As already indicated above, many aspects of the proposed large-scale microalgae production process require R&D. For example, the individual growth ponds are over ten times larger than present experience. The hydraulics and wind effects in such large ponds must be determined. Major design factors are the depth of the CO_2 supply sumps (which determines CO_2 transfer efficiency), the pond mixing velocities (typically 20 - 30 cm/sec), the number of carbonation stations (a function of CO_2 storage, pH range, outgassing rates), and depth of the pond culture (typically 20 to 30 cm). These factors are interactive and must be optimized. Bioflocculation, a well known natural process which has also been observed in waste grown algae (Benemann et al., 1980), needs to be demonstrated in actual microalgae production. The extraction and processing of the vegetable oils from the algal biomass was cost estimated based on soybean processing, as no relevant data for algal ass is available. Conversion to biodiesel was not included in the cost estimates. The algal oils would be produced by limiting the algal cultures for nitrogen, which has been demonstrated at the laboratory scale but not yet in large outdoor ponds. Also, the assumption is made that desirable algal species can be cultivated in open ponds, with minimal losses due to grazing, predation, diseases, contamination. The development of the techniques for maintaining healthy, productive cultures in large-scale systems requires considerable work. Most important, two productivities are assumed, corresponding to about 5 and 10% solar energy conversion efficiencies at favorable sites in the U.S. The lower productivity is based on what is believed to be achievable with present experience. Approaching the higher productivity, essentially the theoretical limit, will require the development of greatly improved algal strains that, among other attributes, have a lower pigment content, allowing better light utilization in dense cultures (Benemann, 1990).

If close to theoretical productivities are indeed achievable, and the other technical assumptions on which this cost estimates are based verified, then such a process could utilize flue gas CO_2 and produce fuels at about $40/barrel of oil, if a CO_2 mitigation credit of about $60/ton C were provided. This is within the range of CO_2 credits discussed for greenhouse gas mitigation (Lashoff and Tirpak, 1989) and projected future oil prices.

A major constraint on such systems, besides the R&D issues, is the availability of sufficient land and water near the power plant. Each megawatt of power plant capacity would require between 6 and 12 ha. Thus several thousand hectares would be required for a large conventional power plant. Also, only about 30% of the CO_2 emissions from the power plant could be captured, as the system would be sized to utilize most of the CO_2 produced during peak summer daytime algal productivity and CO_2 utilization, wasting night and much of the winter CO_2 outputs. However, even a 30% CO_2 capture would greatly reduce the potential for adverse effects of CO_2 released from such a power plant (Benemann, 1992). And the land area required is a small fraction, less than one tenth, that required for other biomass systems (e.g. tree farms). And such systems would provide over 3,000 barrels of liquid transportation fuels per year per megawatt of power. Thus, in principle, such a process could have merit in the mitigation of power plant CO_2.

FUTURE DEVELOPMENTS IN MICROALGAE CO_2 MITIGATION.

A precedent for microalgae derived fuels exists: small deposits of oil were recovered earlier this century in Australia from the shores of several lakes. The oil derived from hydrocarbons produced by the microalga Botryococcus, which can produce over 60% of its dry weight as pure hydrocarbons of near diesel quality, which washed ashore, leaving hydrocarbons as oily remains on the beaches (Wake and Hillen, 1980). Perhaps it would be possible to mimic such a process under more controlled conditions.

Strong support for the contention that it is possible to produce microalgae in large-scale outdoor systems with low cost processes comes from recent experience with commercial and pilot plants. At Earthrise Farms, Inc. (S. Calif.), a paddle wheel mixed, unlined earthen pond of about 5 hectares has been successfully operated for Spirulina production. In New Mexico, a comparison between plastic lined and unlined 0.1 ha ponds revealed no significant difference (Weissman and Tillett, 1992). Also at this site, several species of diatoms and green algae were maintained for several months as near unialgal cultures at relatively high productivities using brackish waters (Weissman and Tillett, 1989).

Over the past decade, microalgae culture has advanced from small-sale pilot plant operations to full-scale commercial enterprises (Table 1). The utilization of microalgae in wastewater treatment is also advancing, with some channelized, raceway type systems being found in California, where they were pioneered by Prof. W.J. Oswald, of the University of California at Berkeley (Oswald, 1988). Indeed, microalgae waste water treatment systems could be a potential sink for CO_2, including CO_2 from power plants, rather than a CO_2 source as are conventional wastewater treatment plants.

In conclusion, although much R&D is still needed, no insurmountable problems are apparent and no "breakthroughs" are required for the development of low cost microalgae production systems. Thus, microalgae may become an option for CO_2 removal from flue gases and conversion to fuels. Due to resource limitations (the requirement for low cost land and water near power plants), such systems are not likely to provide a major solutions to this problem. Indeed, when considering limitations due to climate, land and water availability, and other factors, such systems could only reduce overall U.S. fossil fuel derived CO_2 emissions by a small percentage, possibly 1 to 2%. However, even such at first glance negligible impacts, represent a significant contribution to the overall effort of containing CO_2 emissions. There are many different, small-scale, approaches to the reduction in CO_2 emissions, providing a continuum of options of increasing costs. Another factor are the powerful self-cleaning capabilities of the earth system (almost half of the total CO_2 emitted to the atmosphere by human activity disappears into poorly known sinks). Thus, the goal of CO_2 mitigation need not reach a 100% of fossil fuel emissions, and even modest reduction in CO_2 emissions can have large effects on prospective climate changes. Any technology that can reduce even a modest fraction of total CO_2 emissions could have disproportionate impact on future climatic trends.

REFERENCES

Benemann, J.R. 1990. "The Future of Microalgae Biotechnology" In R.C. Cresswell, T.A.V. Rees, and N. Shah, eds., *Algal and Cyanobacterial Biotechnology*, 317 - 337 Longman, London.

Benemann, J.R.. 1992. "The use of Iron and other Trace Element Fertilizers in Mitigating Globla Warming", *Plant and Soil*, 15: 2277 - 2313.

Benemann, J.R., and D.M. Tillett. 1987. "Microalgae Lipid Production". In D. Klass, ed., *Symp. Proc. Energy from Biomass and Wastes XI*, Institute of Gas Technology, Chicago, Illinois.

Benemann, J. R., B. L. Koopman, J. C. Weissman, D. E. Eisenberg and R. P. Goebel. 1980. "Development of Microalgae Harvesting and High Rate Pond Technology". In G. Shelef and C. J. Soeder, eds. *Algal Biomass*, 457 - 499. Elsevier Biomedical Press, Amsetrdam.

Benemann, J.R., R.P. Goebel, J.C. Weissman, D.C. Augenstein. 1982. *Microalgae as a Source of Liquid Fuels*, Final Report U.S. Department of Energy, pp. 202.

Burlew, J., ed. 1953. *Algae Culture: From Laboratory to Pilot Plant*, Carnegie Institute, Washington D.C.

Lashof, D.A., and D.A. Tirpak. 1989. *Policy Options for Stabilizing Global Climate.* U.S. Environmental Protection Agency, Washington D.C.

Neenan, B., D. Feinberg, A. Hill, R. McIntosh, and K.Terry. 1986. *Fuels from Microalgae: Technology Status, Potential, and Research Requirements.* Solar Energy Research Institute, Golden Co., SERI/SP-231-2550.

Oswald, W.J., and C.G. Golueke. 1960. *Adv. Appl. Microbiol.*, 11: 223 - 242.

Oswald, W.J. 1988. "The Role of Microalgae in Liquid Waste Treatment and Reclamation". In: Algae and Human Affairs, C.A. Lembi and J.R. Waaland, eds., Cambridge Univ. Press.

Wake, L.V., and L.W. Hillen. 1980. "Study of a Bloom of the Oil-rich Alga Botryococcus braunii in the Darwin River Reservoir". *Biotech. Bioeng.*, 22: 1637 - 1656.

Weissman, J. C. and R. P. Goebel. 1987. *Design and Analysis of Pond Systems for the Purpose of Producing Fuels*, Solar Energy Research Institute, Golden Colorado SERI/STR-231-2840.

Weissman, J.C. and D.T. Tillett, 1989. "Design and Operation of an Outdoor Microalgae Test Facility". In W.S. Bollmeier and S. Sprague, Eds. *Aquatic Species Program, Annnual Report*, 41 - 58. Solar Energy Research Institute, Golden Co., SERI/SP-231-3579.

Weissman, J.C. and D.T. Tillett. 1992. "Design and Operation of an Outdoor Microalgae Test Facility: Large-Scale System Results", L.M. Brown and S. Sprague, Eds. *Aquatic Species Project Report*, FY 1989 - 1990, pp. 32 - 56 National Renewable Energy Laboratory, Golden Co., NREL/MP-232-4174.

The following manuscript was unavailable at the time of publication.

MAKING CHEMICALS FROM CO_2

E. Lipinsky
Battelle Columbus
505 King Avenue
Columbus, OH 43201

Please contact author(s) for a copy of this paper.

The following manuscript was unavailable at the time of publication.

EXPERIMENTAL DESIGN FOR COMPARISON OF TOXIC EMISSIONS FROM UTILITY COAL-FIRED BOILERS WITH AND WITHOUT LOW NO_x BURNERS TO EMISSIONS FROM A LABORATORY SCALE COMBUSTOR

G. Sverdrup
Battelle Columbus
505 King Avenue
Columbus, OH 43201

Please contact author(s) for a copy of this paper.

A STUDY OF TOXIC EMISSIONS FROM A COAL-FIRED POWER PLANT

DEMONSTRATING THE ICCT CT-121 FGD PROJECT

O.W. HARGROVE, JR., PROJECT MANAGER
D.P. MAXWELL, SENIOR SCIENTIST
W.A. WILLIAMS, SENIOR SCIENTIST
H.B. FLORA, PROJECT MANAGER
RADIAN CORPORATION
AUSTIN, TX

M.D. DURHAM, VICE PRESIDENT
ADA TECHNOLOGIES
ENGLEWOOD, CO

Introduction

The U.S. Department of Energy is performing comprehensive assessments of toxic emissions from eight selected coal-fired electric utility units. These data are being collected in response to the Clean Air Act Amendments of 1990, which require that EPA conduct a study of the emissions of hazardous air pollutants (HAPs) from electric utility power plants, and these emissions be evaluated for potential health risks. The data will be compiled and combined with similar data that are being collected as part of the Field Chemical Emissions Monitoring program sponsored by the Electric Power Research Institute (EPRI) and will then be furnished to the U.S. Environmental Protection Agency for emissions factor and health risk determinations.

The assessments of emissions involve the collection and analysis of samples from the major input and output streams of each of the eight power plants for selected hazardous pollutants contained in Title III of the Clean Air Act. Additional goals of these assessments are to collect data from the selected plants that may be helpful in characterizing removal efficiencies of pollution control subsystems for these selected pollutants and to determine the concentrations associated with the particulate fraction of the flue gas stream as a function of particle size. Material balances will be performed for selected pollutants around the entire power plant and numerous subsystems to determine the fate of hazardous substances in each utility system and to provide an overall check on data quality.

Radian Corporation was selected to perform one toxics assessment at a plant demonstrating an Innovative Clean Coal Technology (ICCT) Project. The selected site is the Plant Yates Unit No. 1 of Georgia Power Company, which includes the ICCT CT-121 demonstration project.

Site and Process Descriptions

Plant Yates Unit No. 1 is a bituminous coal-fired steam electricity-generating unit with a net generating capacity of 100 MW. Located in Newnan, Georgia, the station is owned and operated by Georgia Power Company. The station uses a tangentially fired boiler that burns a 2.5%-sulfur blend of Illinois No. 5 and Illinois No. 6 bituminous coals. An electrostatic precipitator controls particulate matter, and the Chiyoda Thoroughbred-121 process controls sulfur dioxide emissions from the entire flue gas stream. Figure 1 shows a process schematic.

The ESP is a conventional weighted wire configuration typical of many of the older ESPs found on coal-fired utility boilers in the midwest and Eastern parts of the United States. The specific collection area is 210 ft^2/kacfm at full load. This size is representative of the ESPs built during the 1970s to provide collection efficiencies of 95 to 99%.

The Chiyoda Thoroughbred-121 is a second-generation flue gas desulfurization (FGD) process employing a unique absorber design, called a jet bubbling reactor (JBR), to combine conventional SO_2 absorption,

neutralization, sulfite oxidation, and gypsum crystallization in one reaction vessel. The process is designed to operate in a pH range of 3 to 5, where the driving force for limestone dissolution is high, resulting in nearly complete reagent utilization. Oxidation of sulfite to sulfate is also promoted at the lower pH because of the increased solubility of innate oxidation catalysts such as iron. Because all the absorbed SO_2 is oxidized, there is sufficient surface area for gypsum crystal growth to prevent the slurry from becoming significantly supersaturated with respect to calcium sulfate. This significantly reduces the potential for gypsum scaling. This design eliminates the need for large recirculation pumps which can damage gypsum crystals and negatively effect gypsum dewatering properties.

The gas-liquid contacting in the JBR is quite different from other commercial FGD processes. The JBR forces flue gas beneath the surface of the scrubbing slurry through sparger orifices. As a result, bubbles are formed as the gas rises through the slurry, creating a froth zone. As bubbles form and then collapse, intimate gas-liquid contact occurs which enhances both SO_2 and particulate removal efficiencies.

Overview of Results

Radian's approach to meeting the test objectives utilized established sampling methods (where possible) and a sampling strategy consistent with that of the EPRI-sponsored FCEM project. Samples were collected with the boiler operating within 10% of full load, at steady-state conditions, and in triplicate over two periods of three days each: June 21-23 (organic species) and June 25-27 (inorganic species), 1993. This paper focuses on the inorganic results. Material balances, removal efficiencies, and emission factors were calculated from the process and analytical data collected at Yates. Calculated results rely on measurement data that are near or below the analytical detection limit for many of the substances of interest. Uncertainty analyses and calculation of confidence intervals were included in the project to quantify the level of uncertainty.[1] The following items summarize some of the important observations:

Material balances were calculated around the boiler, ESP, JBR, and total plant for 27 elements. Figure 2 shows results of the overall plant closures. Of the 27 elements, 16 met the project target of 70 to 130% closure around the entire plant. A total of 24 of the elements had closures of 50% to 150%. Arsenic, molybdenum, and phosphorus did not. The arsenic coal analyses by GFAA yield mass balance closures of 214% and 270% around the boiler and plant, respectively. When INAA data for coal analyses were used, the closures were 103% and 134%, respectively. This suggests that the GFAA analysis performed for coal may have been biased.

Emission factors were calculated for 15 metals as shown in Table 1. Emission factors for these metals are generally on the lower end of the ranges reported by EPA in 1989.[2]

Removal efficiencies were calculated for both the ESP and JBR and are presented in Table 2. The total particulate removal efficiencies of ESP and JBR were 98.4% and 90%, respectively. The removal efficiencies of most metals (both vapor and particulate phases) across the ESP were in the 95% to 99% range, which is reasonable since most of the metals exist primarily in particulate phase at 300°F. With the exception of Mo (analytical difficulties previously discussed), the substances whose removal efficiencies did not fall in this range are those expected to have significant vapor-phase components. A number of the substances showed greater than 90% removal across the JBR. The performance of each of these control devices is discussed in more detail in subsequent sections of this paper.

Comparison of vapor and particulate composition. Most of the inorganic substances at Plant Yates are distributed between the flue gas (vapor) and the particulate matter associated with the bottom ash, collected ash, ash removed in the FGD system, or emitted ash which exits with the flue gas through the stack. At the ESP temperature, more than 99% of most substances were in the particulate phase. Exceptions are chloride, fluoride, selenium, and mercury. With these same exceptions, the particulate phase is the predominant phase at the ESP outlet and stack.

Extractability of metals from fly ash surfaces was determined using nitric acid (EPA SW 3050), simulated gastric fluid, and TCLP leaching solutions. Metal solubility, particle surface area, surface concentration, and other matrix effects can influence the leachability of metals from particles. Increasing extractability was generally observed along the flue gas path, and, in general, metals which are most enriched in the finer ash sizes were also more leachable as shown in Figure 3. However, Figure 3 shows the "average" leachability for the three leaching solutions which does not adequately convey differences among metals. Figure 4 shows that different metals exhibit different leachabilities for the different solutions. For example, a fairly high fraction of Cd is leached by all three solutions, while the fraction Cr leached is fairly low for all solutions. On the other hand, As is highly leachable in nitric acid but is not leached to a great extent with the gastric fluid or TCLP leaching solutions. As health risk assessments are being conducted, the surface availability and leachability in biological processes should be more closely examined.

ESP Performance

Figure 5 shows particulate penetration as a function of particle size, with both actual measured data and predicted results. The predictions in Figure 4 were derived from a computer model developed by ADA for DOE displayed. The modeled results compare well with actual data which indicate that the ESP was functioning as expected for the fly ash and flue gas conditions present . The total particulate penetration was 1.6% (98.4% removal), but the penetration is particle size dependent with the maximum penetration of 6 to 8% occurring in the 0.2 to 0.8 μm size range. Less than 0.8% of the particles 10 μm and larger penetrated the ESP. A point to emphasize here is that, while the fraction of submicron particles that penetrate the ESP was a factor 10 greater than the large particles, more than 92% of the submicron particles were collected.

Figure 6 shows the relative concentrations of the metals according to particle size for the ESP inlet. (If the concentration were exactly the same in each size fraction, the normalized concentration in Figure 6 would be 33.3%.) The fraction of each particulate size range relative to the total particulate loading is shown as well. Figure 6 shows that most elements are fairly well distributed through all size fractions and should be removed relatively efficiently by a well operating ESP. A few metals (e.g., As) have relatively higher concentration in the <3 μm fraction and would, therefore, be expected to penetrate the ESP to a greater extent than metals that are more uniformly distributed (e.g., Al).

Figure 7 shows ESP penetration as a function of metal species with the total penetration shown for reference. There are several elements that have a higher penetration than the 1.6% for the total particulate matter. The most notable of these is Se with 60% penetration which does not appear to be a reasonable result. Even if all the Se were in the 0.2 to 0.8 μm size range, a maximum of 8% penetration would be predicted based on the model of ESP performance. Sampling or analytical artifact is believed to be the cause of the high Se penetration value. Arsenic (4%), cadmium (4.5%), and phosphorus (4.8%) also have relatively high but reasonable penetration values. Figure 5 shows that these latter three metals are relatively enriched in the <3 μm size fraction in the ESP inlet stream.

JBR Performance

The JBR is also an effective particulate control device which achieves an additional 90% reduction in total particulate matter. The resulting particulate loading in the stack gas is only 0.006 gr/dscf. Closer examination of the composition of the particulate caught on the filter suggests that about 67% of the stack particulate matter is condensed sulfuric acid (which translates to about 1 to 2 ppm SO_3 if this material were in the vapor phase), about 25% is fly ash penetration, and the remainder is carryover from the FGD system (<10%). Data on the major metals (Al, Fe, Mg, K, Na, and Ti) indicate that about 96% of the fly ash entering is removed from the flue gas in the JBR. (The JBR/ESP combination removes 99.8% of the total particulate matter—greater than 99.9% if adjustment for sulfuric acid on the filter is made.)

Figure 8 shows that most elements penetrate the JBR at rates less than 15% of the ESP outlet rates. Of the exceptions, Cr and Ni had high stack value in the same run which may indicate sample contamination for that

run. Cd is one of the elements that only had one ESP outlet value due to high background on the filters for the other runs. As discussed previously, sampling artifact is suspected in ESP inlet and outlet Se concentrations and perhaps in the stack values as well.

Of the elements which are found predominantly in the vapor phase, the anions, Cl and F, were removed at very high efficiencies, 99 and 98%, respectively. These elements exist primarily as acid gases and are therefore removed efficiently across an FGD system designed to remove another acid gas, SO_2.

Mercury, the other predominantly vapor-phase substance, is removed at much lower efficiency, about 50%, a value much lower than some would expect across a wet scrubber. The reason for the lower removal is probably due to the form of mercury in the flue gas at Yates. Figure 8 shows partitioning of mercury vapor by the Bloom train and in EPA Method 29 (most ionic mercury reports to nitric/peroxide impingers and most elemental mercury reports to the permanganate impingers). The Bloom method resulted in slightly higher elemental mercury values and sightly lower oxidized mercury values, with the total mercury vapor-phase concentrations very similar. If the mercury removal is evaluated according to form (see Figure 9), both methods show relatively high oxidized mercury removal and negative elemental mercury removal (elemental mercury is generated across the JBR). High removal efficiency of the oxidized forms is expected because of their relative solubility in water. Elemental mercury generation is apparently occurring through the absorption of oxidized mercury and subsequent reduction to elemental mercury in the FGD liquid. These results support the theory that the FGD mercury removal efficiency is highly dependent on the form of mercury that exists in the flue gas.

Recommendations and Considerations

Some sampling, analytical, and/or process-related issues were identified during this study that may warrant further consideration. Among these are 1) selenium sampling and analysis, 2) mercury partitioning and speciation, and 3) fly ash penetration. Selenium could not be accurately quantified throughout the process. Apparent problems were associated with both the collection and the analysis of selenium. Further study of selenium is recommended.

Mercury was collected and analyzed by Method 29 and the Bloom method. One phenomenon observed is an apparent increase in the elemental mercury concentration across the FGD system. Another anomaly is the apparent "enrichment" of mercury in fly ash particles when collected from the flue gas via filtration. These two items warrant further study and investigation.

The link between particle size, surface orientation of trace elements, and the penetration of fine particles cannot be demonstrated by comparing the extractable and total metal concentrations of the particulate emissions from the FGD system. Fly ash penetration, sulfuric acid mist condensation, and gypsum slurry carryover add variables to the assessment of air toxic emissions as a function of surface orientation. Controlled condensation test methods should be used in future efforts for measuring sulfuric acid emissions apart from gypsum and SO_2 artifacts. The analysis of tracer elements associated only with the coal ash may be warranted to more accurately determine ash penetration and dilution from scrubber solids. Analysis of size-fractionated particulate emissions could potentially identify the predominant size ranges associated with individual components.

Test efforts to quantify the relative contribution of each source to particulate emissions may be of interest to those considering wet scrubbers for control of air toxics as well as SO_2. These data would provide a basis of comparison between surface extractability of the dry ash entering an FGD system and the particulate emissions downstream.

References

1. "Measurement of Uncertainty," ANSI/ASME, PTC 19.1, 1985.

2. Estimating Air Toxic Emissions from Coal and Oil Combustion Sources, EPA-450/2-89-001, U.S. EPA Office of Air Quality Planning and Standards, RTP, North Carolina, April 1989.

Table 1
Emission Factors

Element	lb/10^{12} Btu	95% CI	Element	lb/10^{12} Btu	95% CI
Antimony	0.4	3.8	Lead	0.6	0.6
Arsenic	1.2	0.2	Manganese	7.2	48
Barium	2.8	1.3	Mercury	3.0	0.3
Beryllium	0.1	0.004	Molybdenum	1.5	3.4
Cadmium	0.6	0.8	Nickel	40.1	435
Chromium	5.3	49.6	Phosphorus	9.4	8.2
Cobalt	0.7	0.8	Selenium	26.5	58
Copper	2.0	2.3	Vanadium	2.1	0.5

Table 2
Removal Efficiencies (Includes Particulate and Vapor Phase)

	ESP		JBR	
	% Removal	95% CI	% Removal	95% CI
Anions				
Chloride	-7.0	47	99	1
Fluoride	1.7	37	98	1
Elements				
Aluminum [a]	98.6	-- [b]	98.4	--
Antimony	98.8	0.6	84.1	3.1
Arsenic	95.9	1.5	92.7	2.1
Barium	98.3	--	96.1	--
Beryllium	98.1	--	92.6	--
Boron [c]	34.3	--	93.5	--
Cadmium	95.1	--	46.2	--
Calcium	98.8	--	85.3	--
Chromium	98.7	--	76.6	--
Cobalt	98.2	--	85.3	--
Copper [c]	97.8	0.3	88.1	13.5
Iron	98.9	0.1	98.0	7.0
Lead	97.4	--	96.7	--
Magnesium	98.4	--	93.3	--
Manganese	98.4	--	78	144
Mercury	55.2 (16.5) [d]	14.4 (20.6) [d]	45.9	7.4
Molybdenum [c]	97.2	2.2	82.5	27.2
Nickel	98.8	0.7	-75.5	1890
Phosphorus [c]	94.8	--	91.1	--
Potassium [c]	98.6	--	96.4	--
Selenium	38.1	85.1	66.9	56.1
Sodium	97.6	--	94.0	--
Strontium [c]	98.5	--	96.6	--
Titanium	98.6	0.4	98.3	0.4
Vanadium	98.0	0.3	96.0	0.9

[a] Spike recovery in ESP inlet gas phase particulate for Al was 62%, indicating possible analytical bias.

[b] Since the ESP outlet gas phase particulate Runs 1 and 3 were discarded, confidence intervals for the ESP and JBR removal efficiencies could not be calculated for many elements.

[c]These elements are consistently enriched in the coal ash over the process stream solid-phase concentrations, suggesting that the coal analyses are biased high for these elements.

[d]ESP inlet gas phase particulate data are suspected to be biased high compared with sluiced ash hopper ash analyses. This is also supported by the high boiler and low ESP mass balance closures. The removal efficiency data in parentheses are calculated with the ESP sluiced ash analyses substituted for the ESP inlet gas phase particulate analyses.

[e]Gas particulate phase data were unavailable. ESP sluiced ash data were substituted.

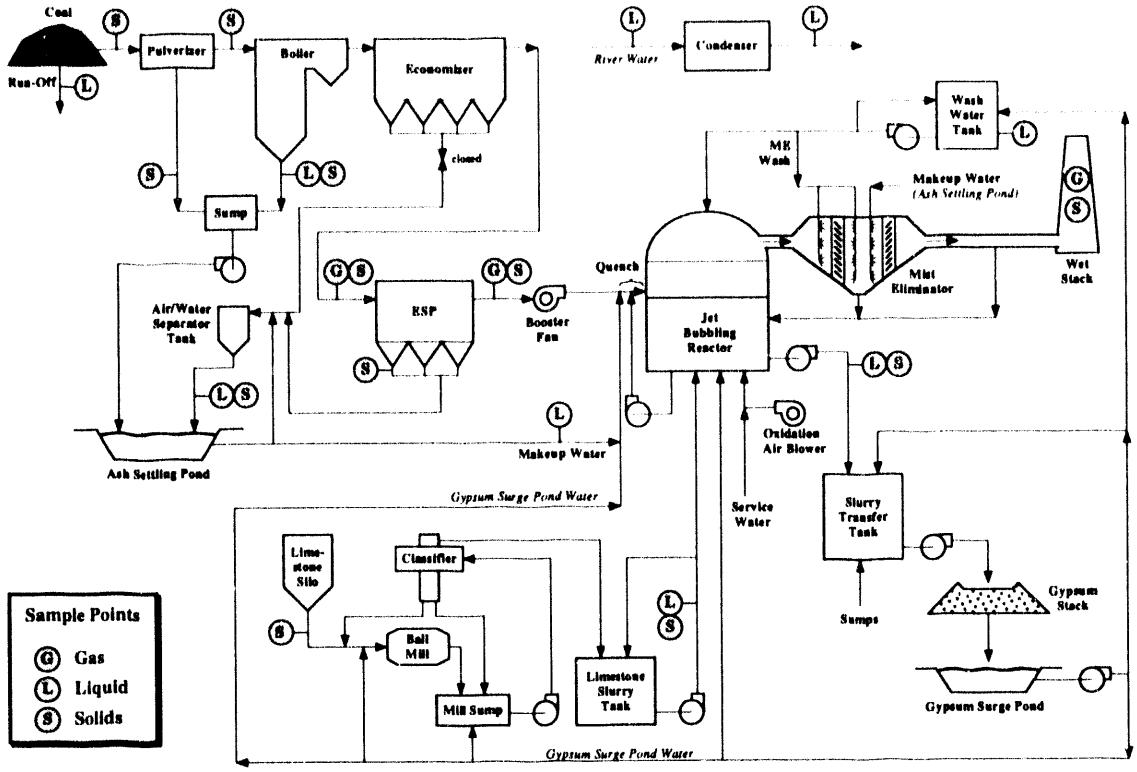

Figure 1. Simplified Process Flow Diagram Illustrating Sampling Locations and Flue Gas Flow

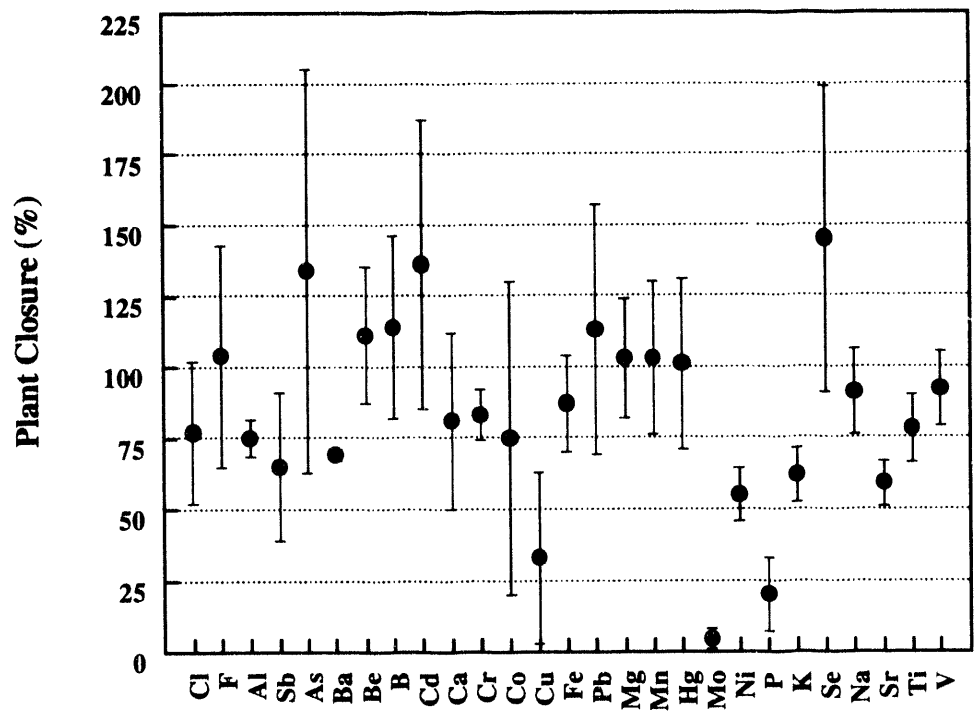

Figure 2. Mass Balance Closures

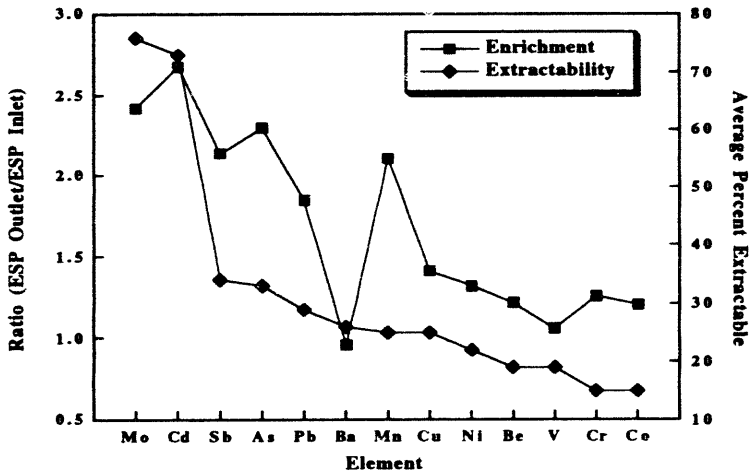

Figure 3. Correlation Between Enrichment and Extractability

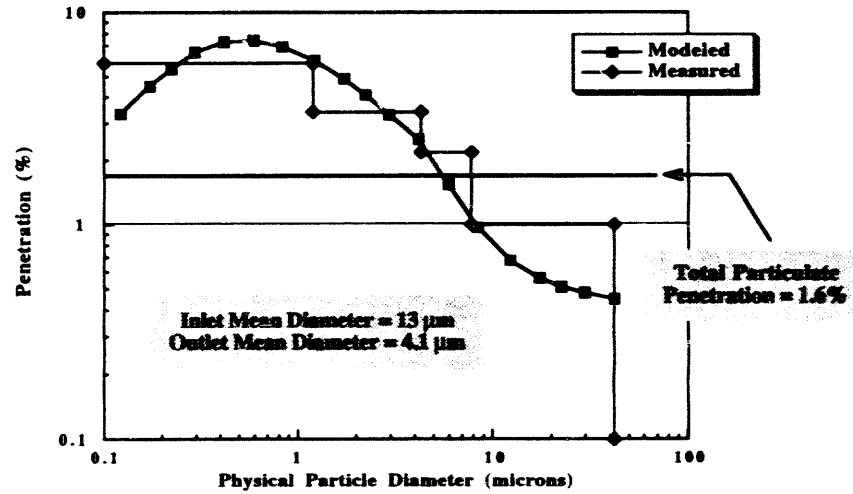

Figure 5. ESP Fractional Penetration Measured vs. Modeled

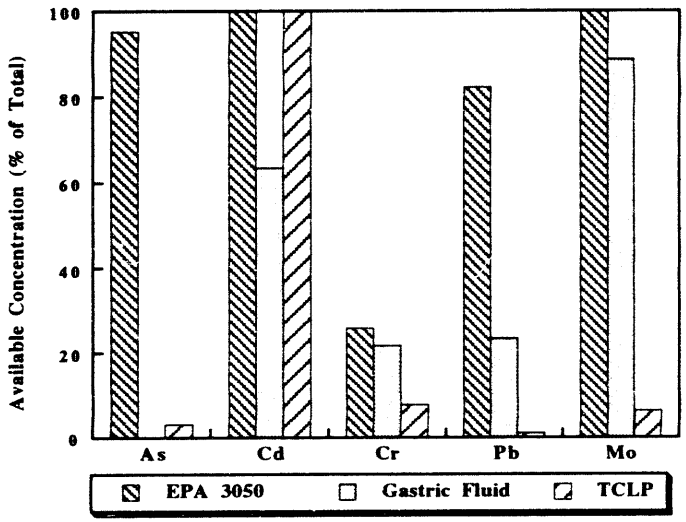

Figure 4. Available Metal Concentration in Particulate Emissions from ESP

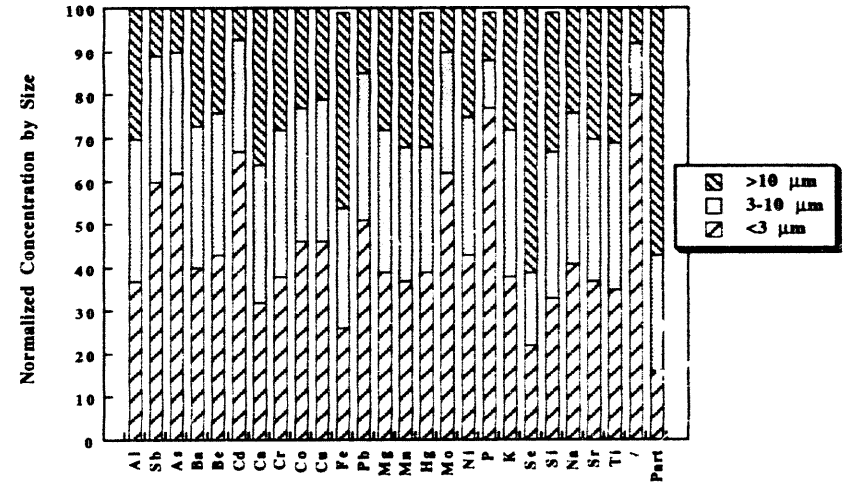

Figure 6. Comparison of Concentrations of Metals as a Function of Particle Size Measured at the ESP Inlet

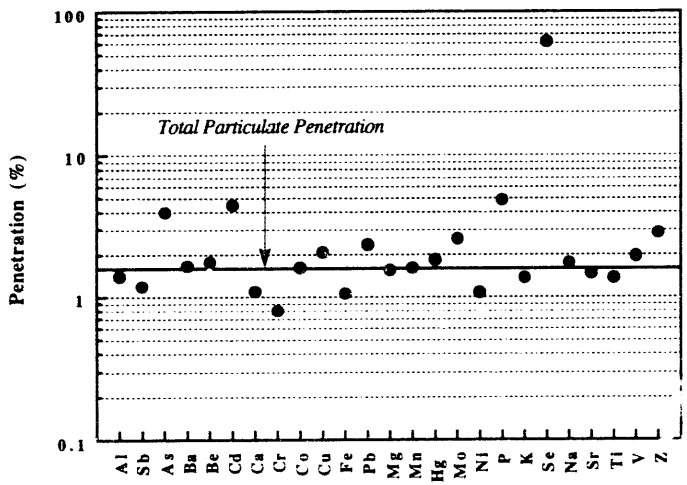

Figure 7. ESP Particulate Metals Penetration

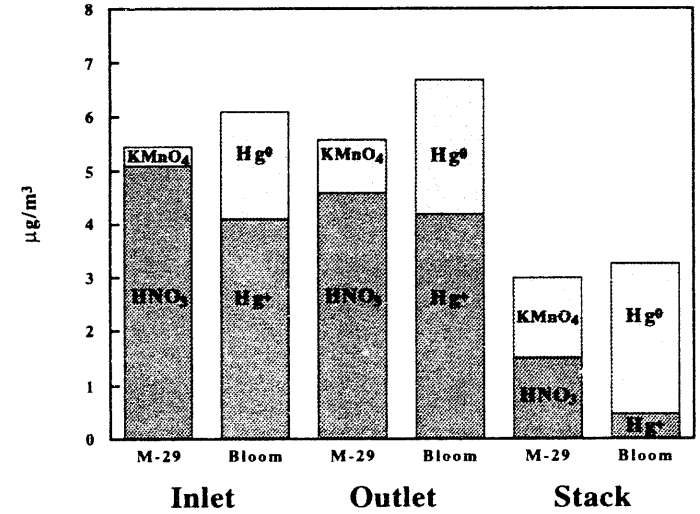

Figure 9. Mercury Vapor Partitioning by Sampling Method

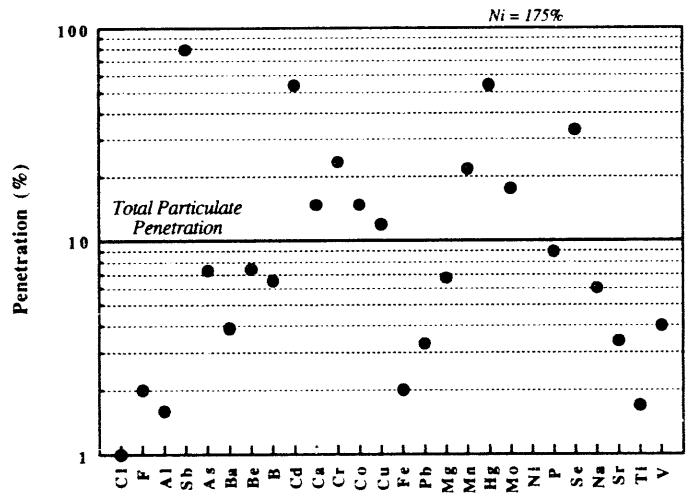

Figure 8. JBR Penetration

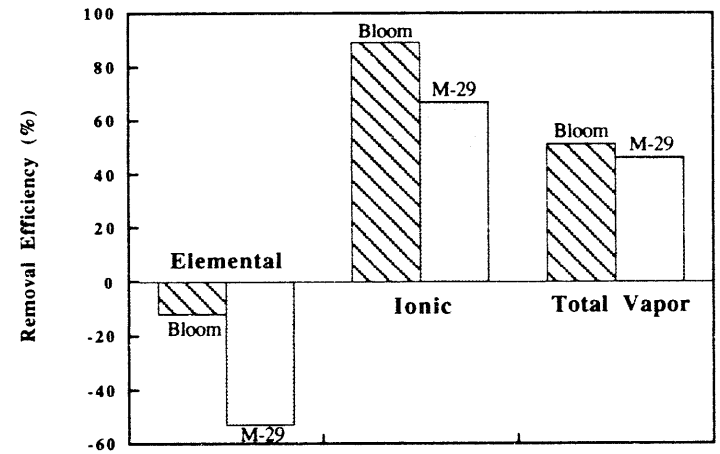

Figure 10. Mercury Removal Across JBR by Sampling Method

MAJOR FINDINGS AND RESULTS FROM COMPREHENSIVE ASSESSMENT OF EMISSIONS FROM TWO COAL-FIRED POWER PLANTS

B.L. JACKSON, PROGRAM MANAGER- ROY F. WESTON, INC. AND
M.S. DEVITO, GROUP LEADER- CONSOL INC. RESEARCH AND DEVELOPMENT

INTRODUCTION

BACKGROUND AND PURPOSE: The U.S. Department of Energy Pittsburgh Energy Technology Center (DOE) sponsored a collaborative effort to characterize toxic emissions and air pollution control equipment (APCE) performance at electric utilities firing bituminous, subbituminous, and lignite coal. This paper presents the major results of the investigative activities of Roy F. Weston, Inc. (WESTON) and its team subcontractors CARNOT, CONSOL Inc. Research and Development, and Triangle Laboratories, Inc. at two of the eight power plant configurations studied by contractors in 1993 under project Phase I: Minnesota Power Company's Clay Boswell Energy Center Unit 2 (Boswell), located in Cohasset, Minnesota, and Illinois Power Company's Baldwin Power Station Unit 2 (Baldwin), located in Baldwin, Illinois.

POWER PLANT AND TEST PROGRAM DESCRIPTIONS

Key information about the configuration and coal source of each plant is shown in Table 1. The coal utilized at each plant was very different in terms of sulfur content, heating value, inherent moisture, and mineral composition. The as-received Powder River Basin (PRB) subbituminous coal fired during the testing program at Boswell averaged 0.70% sulfur, 8,800 Btu/lb heating value, 24.8% moisture, and 8.4% ash. The as-received Illinois Basin bituminous coal burned at Baldwin averaged 2.9% sulfur, 10,600 Btu/lb, 15.0% moisture, and 10.2% ash.

A process flow diagram, with sampling/testing points and material balance boundary identified, is presented in Figures 1 and 2 for Boswell and Baldwin, respectively. At both plants, all potential process sampling/testing sites were evaluated and the optimum location at each process stream location was selected. Site selection factors that were considered included applicable method criteria, the ability to generate representative samples and measurements, and requirements and costs for access, site modifications, sampling equipment, and personnel.

The sampling, testing, and/or analytical method(s) used to determine each pollutant/parameter were standard, reference, or self-validating procedures to promote the attainment of representative data (e.g., 40CFR60, Appendix A- Reference Methods, SW-846, and ASTM). Triplicate tests for each parameter were conducted at each power plant during non-sootblowing periods. Additionally, three sets of tests were conducted during sootblowing periods at Baldwin to investigate the impact of this activity on trace element emissions and APCE performance.

To foster the collection of representative samples under uniform process conditions during testing, prescribed operating conditions were specified for each unit. Each unit was operated near its nameplate rating. Target unit load was established at least two hours prior to testing. After unit load was stabilized at the test load condition, sootblowing and bottom ash and flyash removal were performed prior to commencement of sampling. For both units, testing was representative of normal daily operation near full load during non-sootblowing periods. As mentioned above, testing was also performed during sootblowing periods at Baldwin. All key process operating parameters, including APCE, were monitored and recorded during each test period to provide a meaningful basis for results interpretation.

During testing, the Boswell unit was operated at ~61 MW with an as-fired fuel rate of ~74,000 lb coal/hr. The corresponding heat release rate was ~650 x 10^6 Btu/hr. In this system, the coal combustion residue (CCR) was roughly distributed as 20% bottom ash and 80% overhead ash (i.e., flyash). The measured particulate removal efficiency of the baghouse ranged from 99.8% to 99.9%.

The Baldwin unit was operated between 565 and 575 MW with a corresponding as-fired fuel rate that ranged from 529,000 to 555,000 lb/hr during the test program. This corresponds to a heat release rate range of 5,710 to 5,840 x 10^6 Btu/hr. In this system, the CCR was nominally distributed as 70% bottom ash and 30% overhead ash. Economizer ash collection hoppers located upstream of the ESP removed ~1% of the total CCR. Most of the flyash was collected in the first two ("front half") fields of the ESP and associated ash hoppers. Much of the remaining flyash was removed in the third and fourth ("back half") ESP fields and associated hoppers. The ESP's particulate removal efficiency ranged from 97.1% to 98.1%.

MAJOR FINDINGS AND RESULTS

MATERIAL BALANCES: The average material balance closure results for the 28 major, minor, and trace elements studied at Boswell are presented in Figure 3. Closures for all of the major elements were within the goal range of 100 ± 20%. Closures for 14 of the 18 minor and trace elements were within the goal range of 70% to 130%. Low closures were observed for B, Cl, and Se, while high closures were noted for F. Hg exhibited the largest closure range (50% to 140%).

Comparative results obtained at Baldwin during non-sootblowing periods are shown in Figure 4. The material balance closures for the major elements were all within the goal range, with most closures between 95% and 110%. Balances for 17 of the 18 minor and trace elements were also within the goal range. Se again showed a low balance. This is attributed to either inaccuracies in the coal analyses and/or difficulties in collecting/analyzing Se in the draft EPA Method 29 multimetals train. Once again, Hg exhibited the greatest variability in closure range (55% to 115%).

In general, acceptable material balance closures were achieved at both plants, and the accuracy of sampling and analytical techniques and process stream mass flowrate determinations was confirmed.

MINOR AND TRACE ELEMENT DISTRIBUTIONS: At Boswell Unit 2 there are one major process input and three major process output streams that affect the material balances of interest, specifically: coal feed to boiler; bottom ash; baghouse ash; and stack emissions. The three-test average distributions of minor and trace elements after combustion are shown in Figure 5. The bottom leg of each column indicates the mass percent of that element that was measured in the bottom ash stream. The middle leg indicates the mass percent of the element that was distributed in the baghouse ash stream. The top leg shows the percent reporting in the stack emissions. Ba, Be, Cr, Co, Cu, Mn, Mo, Ni, and V exhibited distributions similar to that observed for the overall CCR (i.e., total ash stream). Elements showing preferential partitioning in the overhead ash were Sb, As, and Pb. Significant amounts of Hg were observed in the baghouse ash. Elements showing significant percent mass in the stack emission stream included Cl, F, As, Cd, Se, and Hg. The material balance closures for B, Cl, and Se were below the goal range and this limited the usefulness of the distribution results for these elements.

Baldwin Unit 2 has one major input and five major output streams that affect the material balances of interest: coal feed to the furnace; bottom ash; bottom ash sluice water; economizer ash; ESP ash; and stack emissions. Elements showing a distribution consistent with the overall CCR were Mn and Ba (see Figure 6). The only element present at significant concentration in the sluice water stream was Cl at about 5% of the total mass of this element. About 1% of the total ash was found in the economizer ash hoppers. No significant elemental enrichments were detected for this process stream. Elements exhibiting a nominal 50:50 total mass split between bottom ash and overhead ash streams were V, Ni, Be, Co, and Cr. Thus, these elements showed mild partitioning, since the approximate bottom ash to overhead ash split was 70%:30%. Elements that indicated greater mass partitioning in the ESP ash stream were Cd, Mo, As, Pb, Sb, and Cu. These elements also showed significant percentages (3% to 6%) of their total mass outputs in the stack emissions. Elements reporting primarily in the stack emissions were Cl, F, Se, B, and Hg.

MINOR AND TRACE ELEMENT PARTITIONING: A continuum scale presenting the ratio of the elemental concentration found in the overhead ash to that found in the bottom ash for Boswell is shown in Figure 7. This ratio defines a simplistic partitioning factor. Ni through Mo show very little partitioning. Se marks the start of a transition where partitioning increases. Elements with measured partitioning factors (PFs) above 2 were Sb, Pb, Cd, and As. The halides reported almost exclusively to the gas stream. The high PF for Hg reflects the relatively high levels of Hg found in the baghouse ash compared to those measured in the bottom ash.

The partitioning of these elements between the overhead ash and bottom ash streams at Baldwin are shown in Figure 8. Little partitioning is indicated for Mn through Ni. Cu marks the start of a transition. Elements exhibiting PFs greater than 5 were B, F, Sb, Mo, Cl, Pb, As, and Cd. Se was below detection limit values, and thus is not included in this data set.

Comparing the results for both plants, elements showing the highest partitioning into the overhead ash stream were Cd, As, Pb, Sb, and Mo. The continuum series for both facilities are similar. Higher partitioning is indicative of elements (and/or their compounds) that volatilize in the furnace and condense in the cooler sections of the process on the smaller overhead ash particles, and is related to elemental or compound volatility.

EFFECT OF SOOTBLOWING: Additional testing was conducted at Baldwin to determine the effect of sootblowing on trace element partitioning. The top graph in Figure 9 shows the enrichment ratio (ER) obtained from samples collected during non-sootblowing periods while the bottom graph depicts the ER results for the tests that were conducted during sootblowing activities. The ER is the ratio of the concentration of an element in the identified overhead ash stream to its concentration in the bottom ash. Both data sets show a consistent enrichment for most elements at the corresponding overhead ash stream sampling location in the utility ash handling system (i.e., increased enrichment is observed at each subsequent ash sampling location). The particle size distribution of the flyash changes at each subsequent stage of collection. Specifically, the mass percent of smaller particles in each subsequent capture increases, because of the higher removal efficiency of the larger particles by the previous collector(s). Elements showing the greatest enrichment were Cd, As, Pb, Cl, Sb, and Mo. These elements are the same elements that exhibited the greatest partitioning between the overhead ash and the bottom ash. Sootblowing resulted in slightly higher enrichment ratios for Sb and As only. Sootblowing had no significant effect on the enrichment of any of the other elements. In other words, these data indicate that there is little change in elemental concentrations in the various output streams between sootblowing and non-sootblowing periods. However, it should be noted that during sootblowing more flyash mass is being transported through the system (i.e., the mass rates of the trace elements are higher). It is also noteworthy that the data indicate good sampling and analytical repeatability, and that the variability previously reported for the material balances is primarily a result of uncertainties in the mass flowrate determinations.

PARTICLE SIZE DISTRIBUTION: At Boswell, three baghouse inlet samples were collected using a three-stage cyclonic separator. Each size fraction was analyzed for the target elements. The top plot in Figure 10 presents the average relative enrichment factors (REFs) determined for five of the elements. The REF is the ratio of elemental concentration in a discrete (smaller) size fraction compared to the largest [i.e., particles >10 micrometers (μm) effective aerodynamic diameter (EAD)] size fraction obtained from the sampler. The results indicate modest enrichments of these elements on the smaller particles. This observation is not surprising and has been well documented in other studies. The bottom graph shows the mass percent of each target element by size range. The results indicate that although enrichment on fine particles is occurring, most of the mass of these trace elements is associated with the larger particles. Less than 10% of the mass of the trace elements is associated with the <1 μm EAD particles, except for Se, in which ~30% of the mass is contained in the submicron size fraction.

Similar elemental enrichment results were obtained at Baldwin (see Figure 11). The results presented are an average of three samples collected. The same trend was observed in each sample. Again, a modest enrichment of trace elements on the smaller particles was observed. The data also show that Sb was preferentially enriched on particles in the 5 μm to 10 μm EAD size range. The lower plot indicates the mass percent of each element in the various size fractions. The data show that approximately 50% of the mass of the listed elements is contained in the largest size fraction and <10% of their mass is found in the submicron size fraction.

TRACE ELEMENT INPUTS AND EMISSION FACTORS: Individual trace element input and output emission factors, expressed in terms of lb/10^{12} Btu, are presented for both power plants in Figure 12. Please note that the Y-axis is logarithmic scale. The PRB coal yielded slightly higher total trace element input rates and higher Cr, Pb, and Mn input mass rates than the Illinois Basin coal. The Sb and Hg input levels were similar in both coals on a comparable heating value basis. The Illinois Basin coal exhibited higher mass input rates for the remaining six elements.

Regarding stack emissions, the Baldwin unit emitted ~3 times the amount of total trace element emissions on a lb/10^{12} Btu basis as compared to the Boswell system. Baldwin exhibited higher individual emissions for all of the trace elements with the exceptions of As (same) and Mn (less).

TRACE ELEMENT REMOVALS: Individual trace element removals for both plants are shown in Figure 13. All of the non-volatile metals showed net removals in the mid- to high-90% range. The baghouse-controlled source operated at an overall particulate removal efficiency of ≥99.8%. The collection efficiency of the baghouse for the target trace elements averaged ~99.2%. The ESP at Baldwin exhibited a particulate collection efficiency that ranged between 97.1% and 98.1%. The total trace element removal by the ESP averaged ~98.2%. In this comparison, the results indicate that the baghouse outperformed or equaled the ESP in every case except for As removal. It must be noted that the particulate removal efficiency of the ESP at Baldwin, which is planned for replacement, does not reflect current state-of-the-art ESP performance. It is expected that a new precipitator, operating at optimum efficiency, should achieve trace element removal efficiencies comparable to those of a baghouse for most species. The mini-graph on Figure 13 presents the measured Hg removals across each system. The Boswell system demonstrated Hg removals approaching 70%, while Baldwin yielded removals of ~28%.

The trace elements exhibiting the highest removal efficiencies were Mn, Ni, and Be. These elements showed some of the lowest partitioning and enrichment attributes. Elements that yielded relatively lower collection efficiencies include As and Cd. These elements showed some of the higher partitioning and enrichment characteristics.

TRACE ELEMENT REMOVAL BY PARTICLE SIZE: The relatively high particulate mass loading in the ESP outlet flue gas stream at Baldwin permitted collection of APCE outlet size fractionated flyash samples. Following analysis of these and the corresponding ESP inlet size fractionated samples, trace element removal efficiencies by particle size range were computed.

The top graph in Figure 14 presents the ESP removal efficiencies for particles >10 μm EAD. The overall removal efficiency for all particles >10 μm EAD was 98.0%. The results reveal that most of the elemental removals were between 95% and 98%. This size fraction represents approximately 75% of the total mass of particulate entering the ESP. Sb and Ni showed the lowest removal rates.

The middle graph shows the fractional elemental removal efficiencies for particles between 5 μm and 10 μm EAD. The overall ESP removal rate for the target trace elements in this size fraction was 95.7%. The individual elemental removals were at this efficiency or higher for all elements except Ni. This size range represents 12% of the total mass of particulate entering the ESP.

The final graph shows removal rates for target species on particles between 1 μm and 5 μm EAD. The overall collection efficiency of the ESP for these elements in this size fraction was 90.1%. Most of the elemental removals were between 85% and 90%. This size range represents about 10% of the total mass of particulate entering the ESP.

The average removal rate of submicron particles, which represent only 3% of the particulate mass entering the ESP, was 86%.

DISTRIBUTION OF TRACE ELEMENT (HAP) EMISSIONS: The primary objective of the power plant studies was to characterize the emissions of hazardous air pollutants (HAPs) from coal-fired utilities. Figure 15 presents a summary of the WESTON Team findings for trace element HAP emissions. Total trace element HAP emissions from Boswell Unit 2 were 0.5 tpy. Of particular note, Mn contributed 72% of the total trace element emissions from this plant. The removal efficiency of this system for Mn was high (>99.3%). The substantial contribution of this element to the overall HAP emission rate was attributable to the relatively high concentration of Mn in the coal feed. Arsenic was the next highest contributor at 12% of the total trace element HAP emissions. At this unit, Hg represented ~2% of the total trace element HAP emissions (=14 lb/year).

Baldwin Unit 2 is >8 times larger than Boswell Unit 2 (568 MW vs. 69 MW). The trace element HAP emissions at Baldwin Unit 2 totaled 6 tpy. Of this, almost half (46%) of the total emissions were attributable to Se and 18% to Cr. Hg comprised ~1% of the total trace element emissions (=120 lb/year) from this unit.

Table 1 - **Utility Descriptions**

Parameter	Minnesota Power Boswell Energy Center Unit 2	Illinois Power Baldwin Power Station Unit 2
MWe Rating	69	568
Firing Mode	Front Wall	Cyclone
Coal Source	PRB	IL Basin
Overhead Ash	~80%	~30%
APCE	Baghouse	ESP
APCE Efficiency	≥99.8%	97%-98%

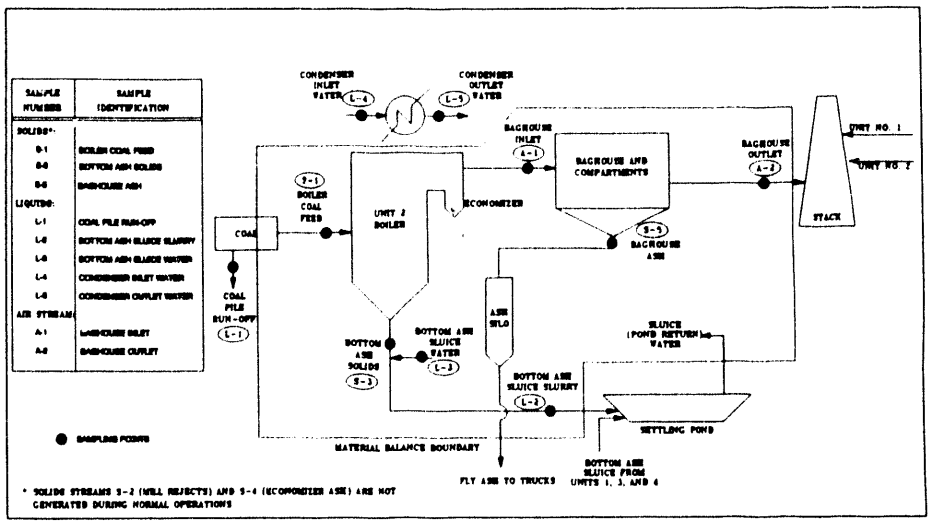

FIGURE 1
PROCESS FLOW DIAGRAM AND SAMPLING/TESTING LOCATIONS OF
BOSWELL ENERGY CENTER UNIT NO. 2

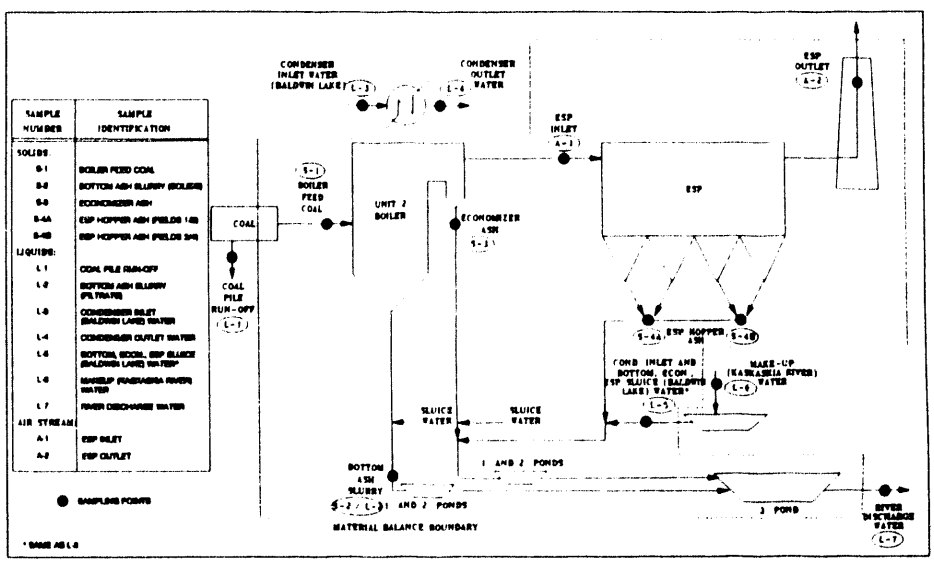

FIGURE 2
PROCESS FLOW DIAGRAM AND SAMPLING/TESTING LOCATIONS OF
BALDWIN POWER STATION UNIT NO. 2

Figure 3

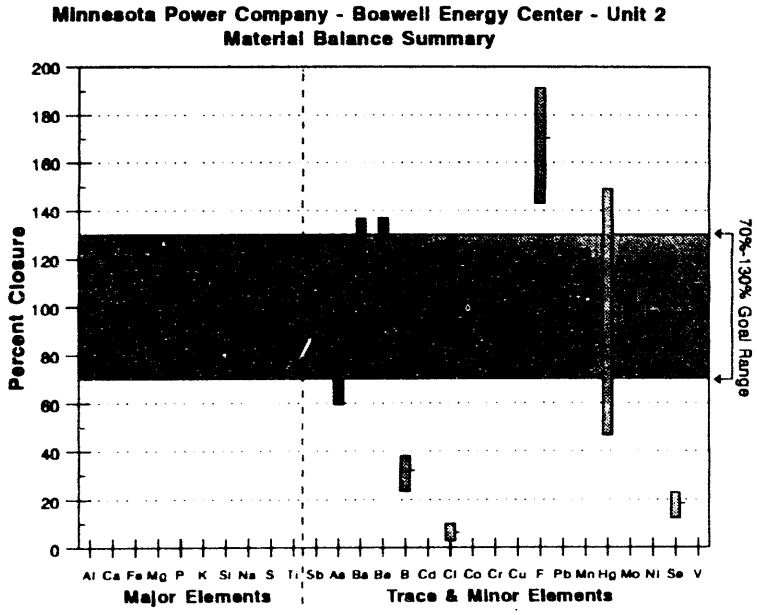

Figure 4

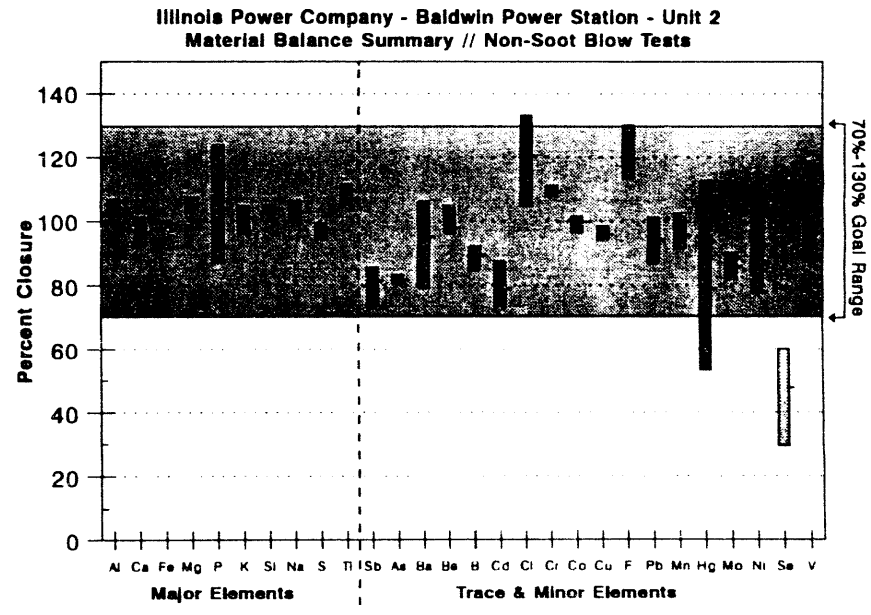

Figure 5

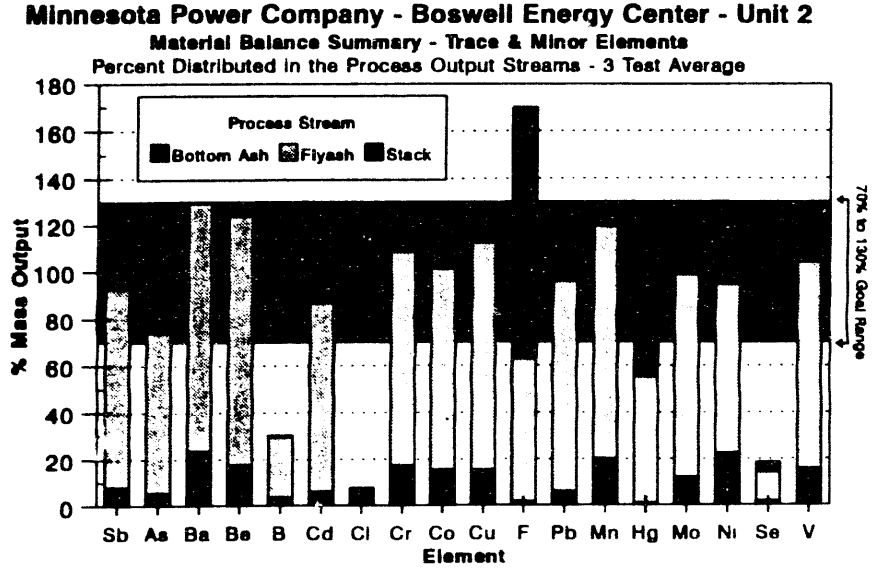

Figure 6

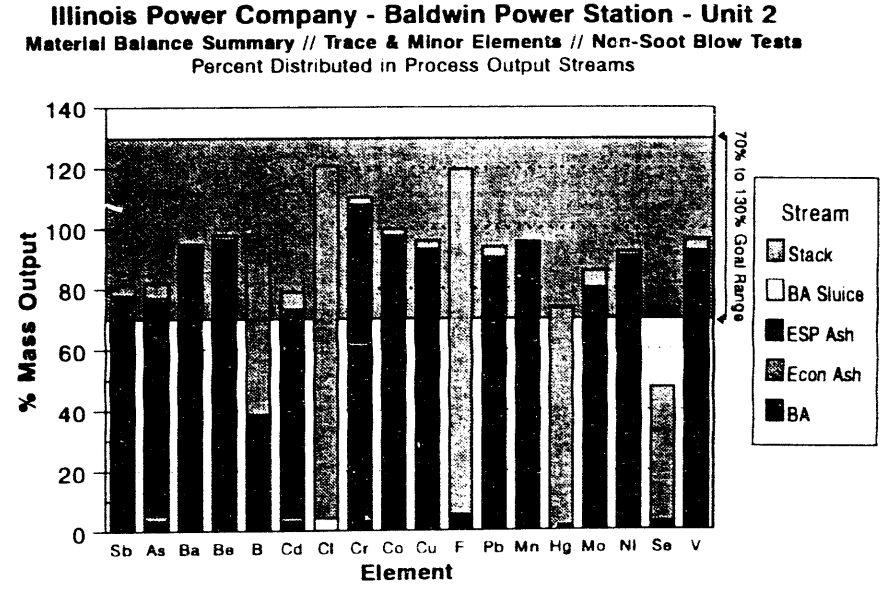

Figure 7

Trace Element Partitioning Factors

Minnesota Power - Boswell Plant

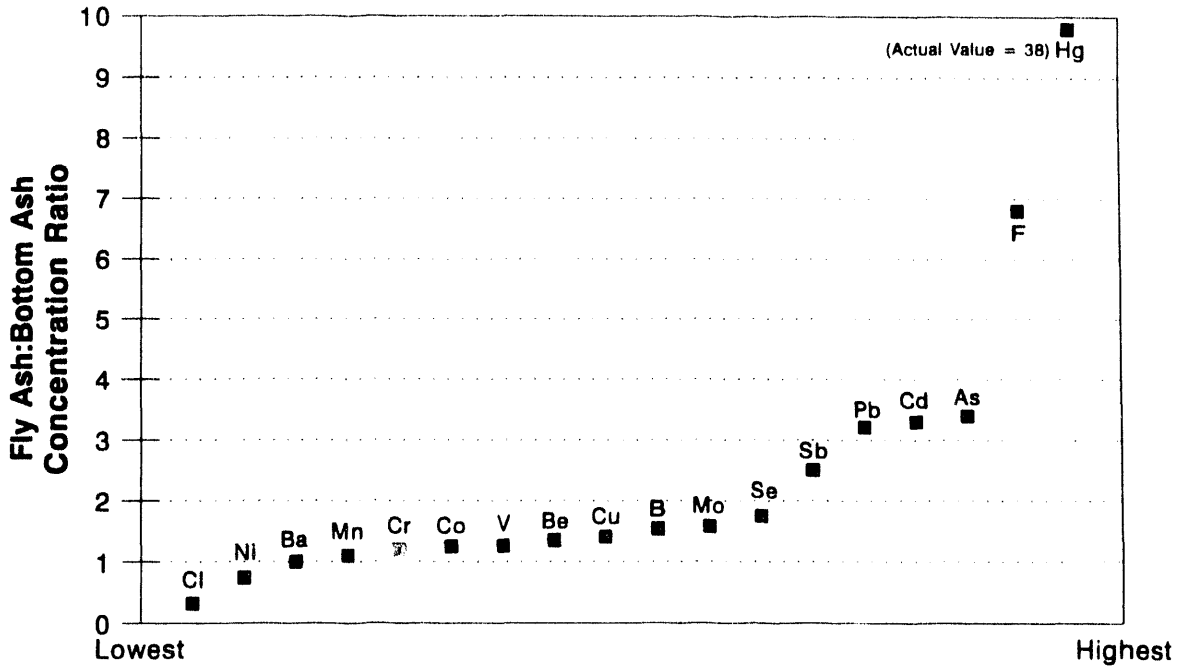

Figure 8

Trace Element Partitioning Factors

Illinois Power - Baldwin Station

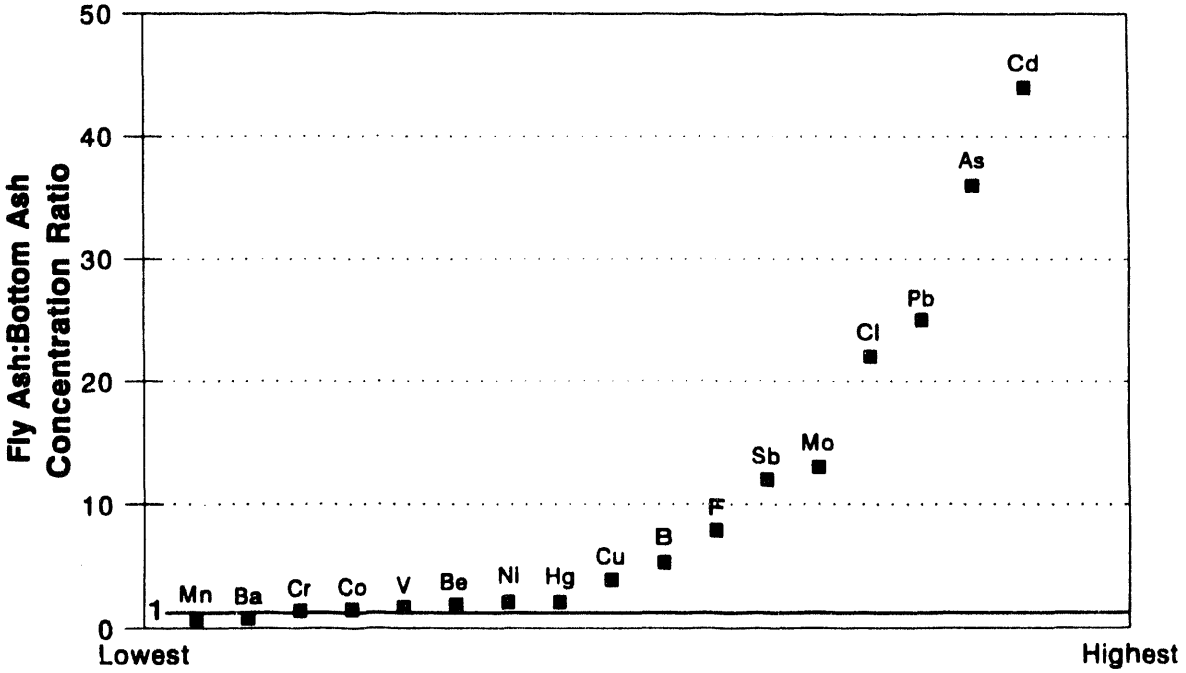

Figure 9

Illinois Power Element Enrichment on Flyash

(Non-Soot Blowing Test Results)

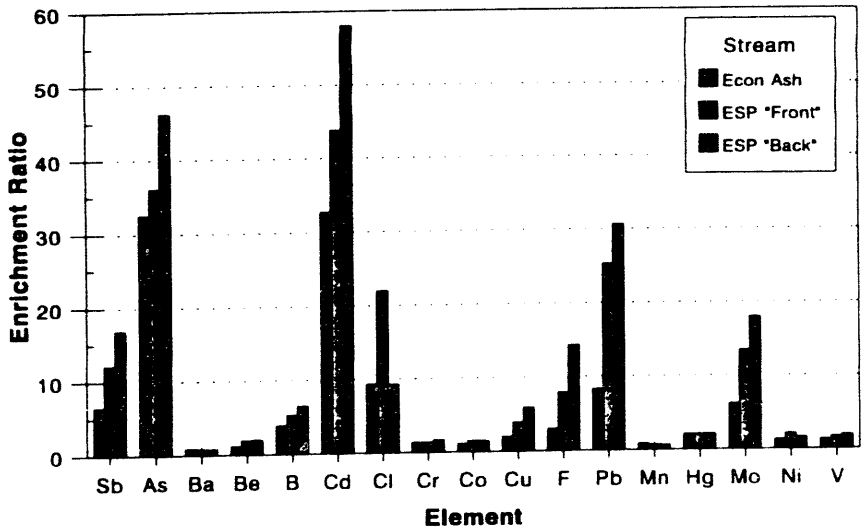

(Soot Blowing Test Results)

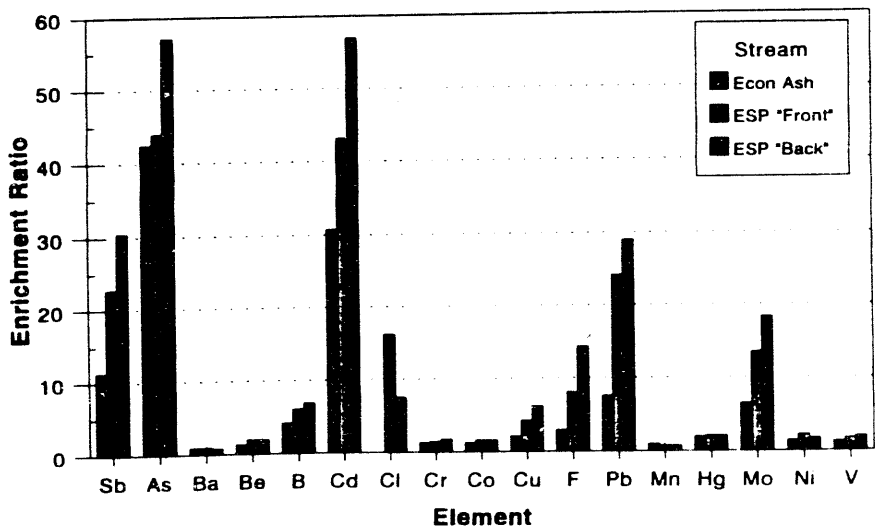

Figure 10

Minnesota Power Company - Boswell Energy Center - Unit 2

Enrichment of Trace Elements by Size

Enrichment of Trace Element By Particle Size

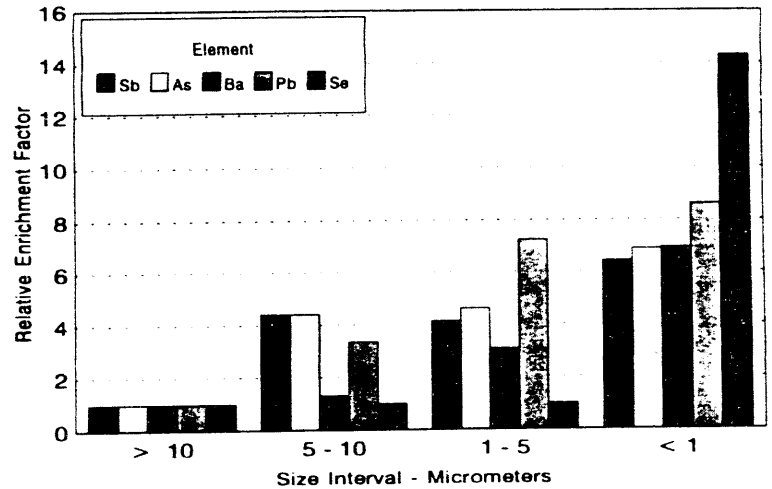

Percent Mass Distribution By Particle Size

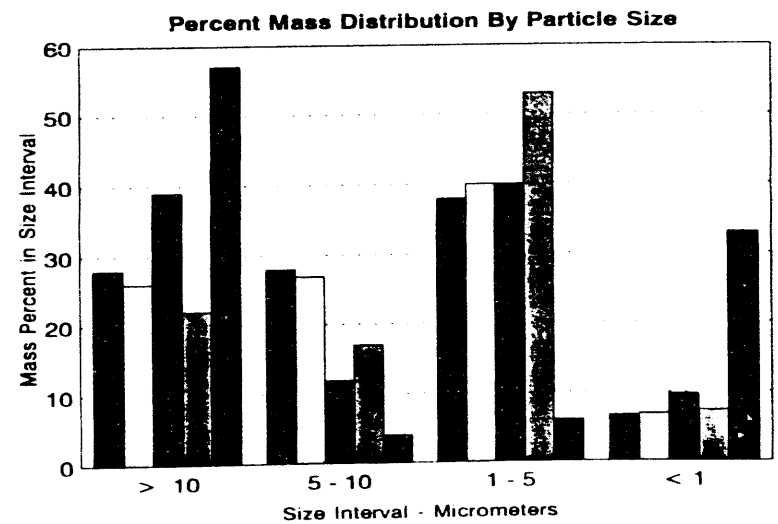

Figure 11

Illinois Power - Baldwin Power Station - Unit 2

Enrichment of Trace Elements by Size

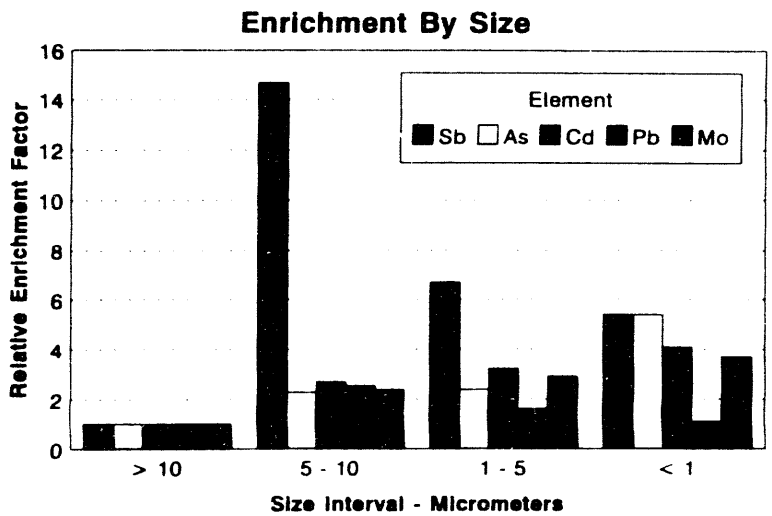

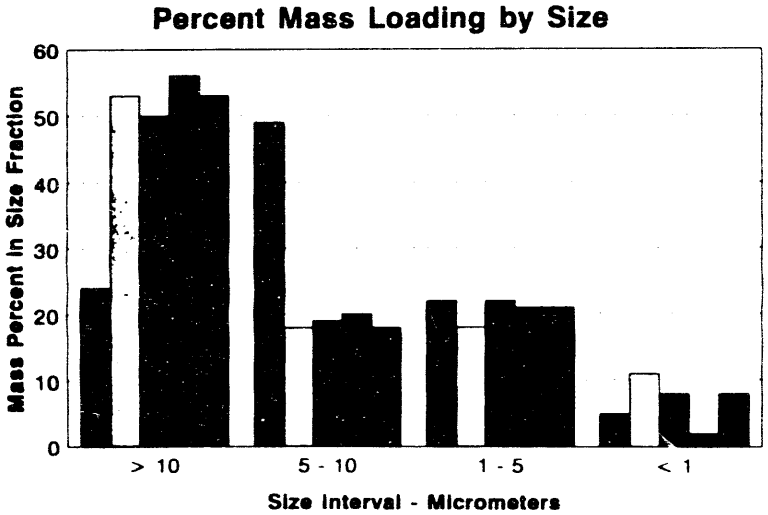

Figure 12

Trace Element Emission Comparison

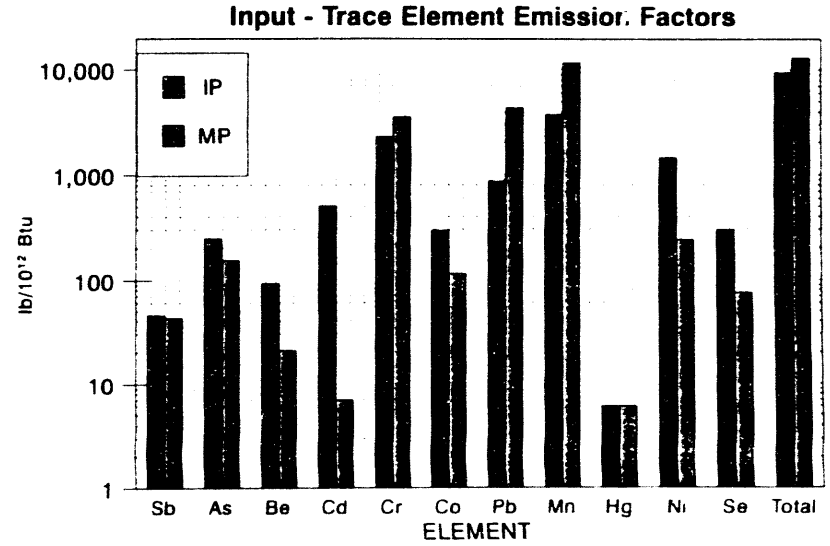

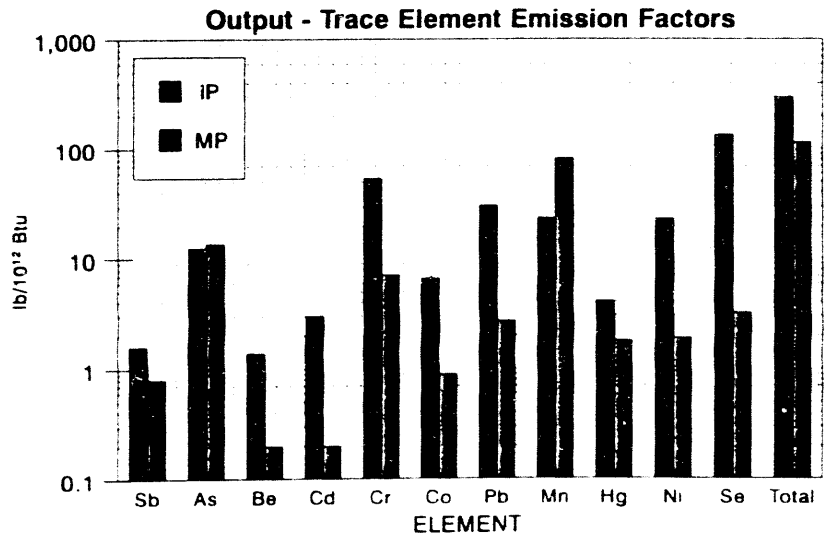

Figure 13

Trace Element Removals Across System

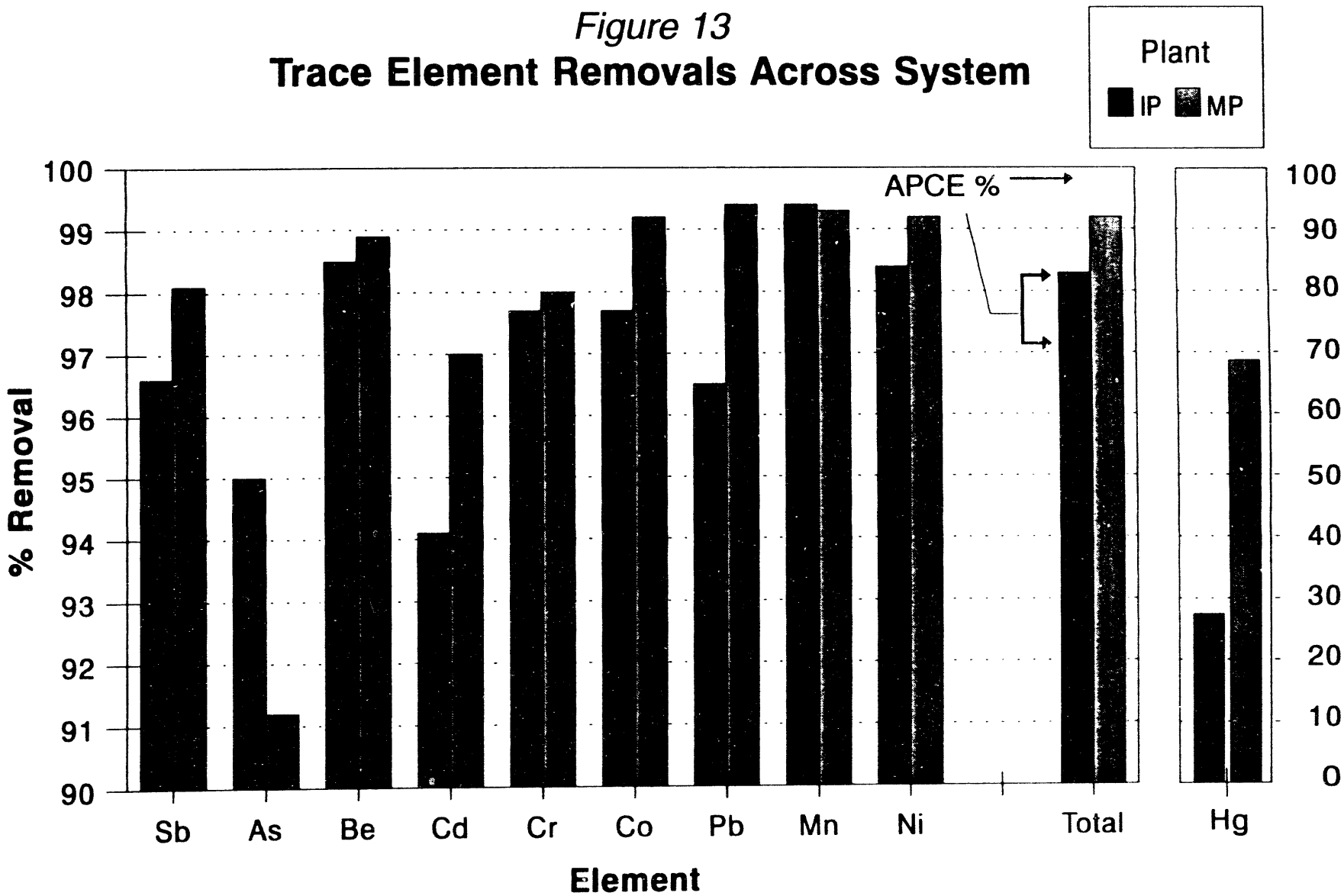

Figure 14

Illinois Power Trace Element Removal by Size

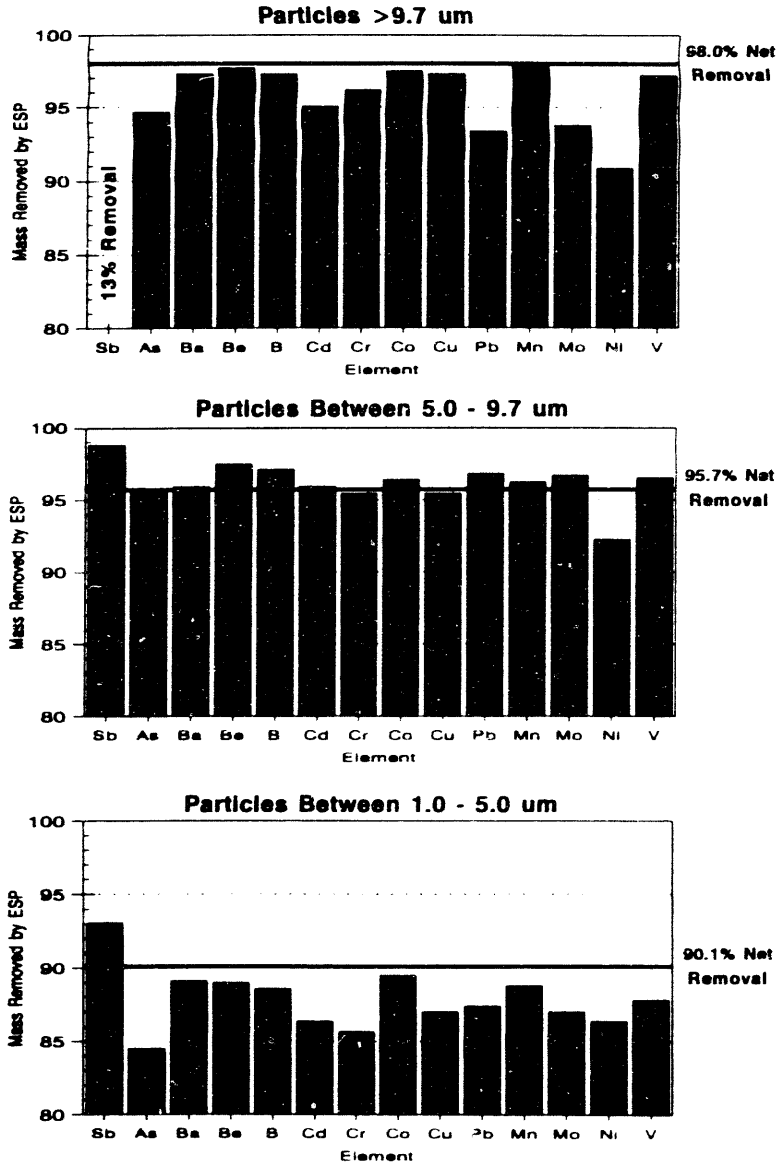

Figure 15

Distribution of Trace Element Emissions

(Elements Identified as HAPs)

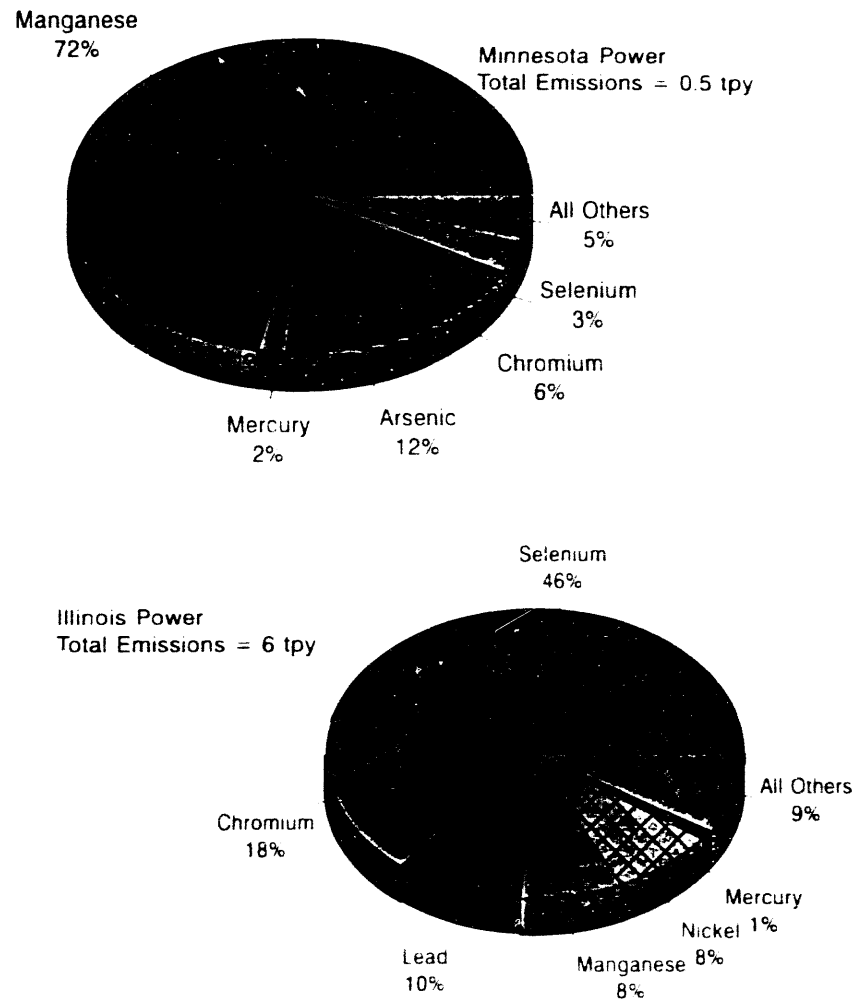

COMPREHENSIVE ASSESSMENT OF AIR TOXICS

AT SPRINGERVILLE GENERATING STATION

E. B. DISMUKES
PRINCIPAL CHEMIST
P. V. BUSH
MANAGER, PARTICULATE SCIENCE AND ENGINEERING GROUP
SOUTHERN RESEARCH INSTITUTE

INTRODUCTION

The DOE's Pittsburgh Energy Technology Center issued a solicitation in February 1992 for Comprehensive Assessment of Air Toxic Emissions to gather data on the presence, control, and emission of potentially hazardous air pollutants (HAPs) at eight different coal-burning electric power stations representing a cross-section of the coals, boiler designs, and emissions control technologies in the United States. Southern Research Institute (SRI) was awarded a contract in April 1993 to assess two of the eight power stations in 1993, with an option to evaluate two more power stations in 1994.

SRI conducted tests at the Springerville Generating Station of Tucson Electric Power Company, the Bailly Generating Station of Northern Indiana Public Service and the associated advanced scrubber system owned and operated by Pure Air, and the Blacksville No. 2 Coal Preparation Plant of CONSOL. Field sampling at the two coal-fired power plants was completed in 1993, and sampling at the coal preparation plant was completed in April 1994.

This manuscript describes the results of the assessment at Springerville Generating Station. This station represents the configuration of NO_x reduction by combustion modification, SO_2 control with a dry scrubber, and particulate control with a baghouse. The test was conducted from June 1 through June 9, 1993.

SAMPLING LOGISTICS

Site Description

Springerville Generating Station is owned and operated by the Tucson Electric Power Company, and is located near Springerville, Arizona. The plant has two identical units that burn subbituminous coal from the Lee Ranch Mine in New Mexico. The coal has an average sulfur content of 0.7% and an ash content of 19%. For each unit typical gross electrical generation at full load is 397 MW, and the net generating capacity is approximately 360 MW. SRI tested Unit No. 2 which began commercial operation in 1990.

The boiler was manufactured by Combustion Engineering (CE), and is a corner-fired, balanced-draft design with overfire air for reducing NO_x emissions. Coal is fed to the boiler

through CE bowl mill pulverizers. Pyrite is separated from the coal in the pulverizers. Unit No. 2 uses a Joy/Niro designed Dry Flue Gas Desulfurization (FGD) system. The system has three spray dryer absorber (SDA) modules, with one atomizer per absorber. A small portion of the flue gas bypasses the SDA modules. The FGD system uses sorbent/ash recycle to supplement fresh lime slurry. Particulate removal is accomplished by two baghouses in parallel downstream of the FGD system. The baghouses exhaust through separate induced draft fans into a 152.4-m tall stack.

Sampling Locations

To assess toxic emissions at the Springerville Generating Station Unit No. 2 required characterizing seven sets of process components:

- Coal - This set includes the run-of-mine coal as the input stream, the conveyer, silos, and pulverizers as the major components, and pulverizer reject and pulverized ash as the output streams.
- Boiler - This set includes the pulverized coal and combustion air as the inputs, and the bottom ash, economizer ash, and flue gas as the output streams.
- Bottom Ash, Economizer Ash, and Pyrite Disposal - This set includes the bottom ash, economizer ash, and pulverizer reject (pyrite) as the input solids and the sluice return water as the input liquid stream, and separate bottom ash sluice and economizer ash and pyrite as output streams.
- Cooling Tower - This set includes the cooling tower makeup water as input and the cooling tower blowdown as the output stream.
- SDA Slurry Preparation - This set includes the lime, service water, baghouse solids, and dilution water (cooling tower blowdown pond water) as inputs, and SDA atomizer feed slurry as the output stream.
- Spray Dryer - This set includes the flue gas, atomizer slurry, and air inleakage as inputs, and flue gas as the output stream. (There is no collection of solids in the SDA modules.)
- Baghouse - This set includes the flue gas from the SDA modules as the input stream and filtered flue gas and collected particulate matter as the output streams.

There were seven solid streams, five liquid streams, three slurry streams, and nominally three flue gas streams (SDA inlet, SDA outlet/baghouse inlet, and stack) from which we collected samples. Because of the duct configurations, the flue gas sampling required measurements in seven ducts at the SDA inlet, four ducts in the SDA outlet, and one elevation at the stack. We also measured the diluted stack gas by sampling through the SRI Condensibles Air Dilution Train at the stack sampling location.

Sample Collection

Triplicate samples were collected for all analytes except for the stack impactor and series cyclones which were run for ~31 and 46 hours, respectively. We used extended

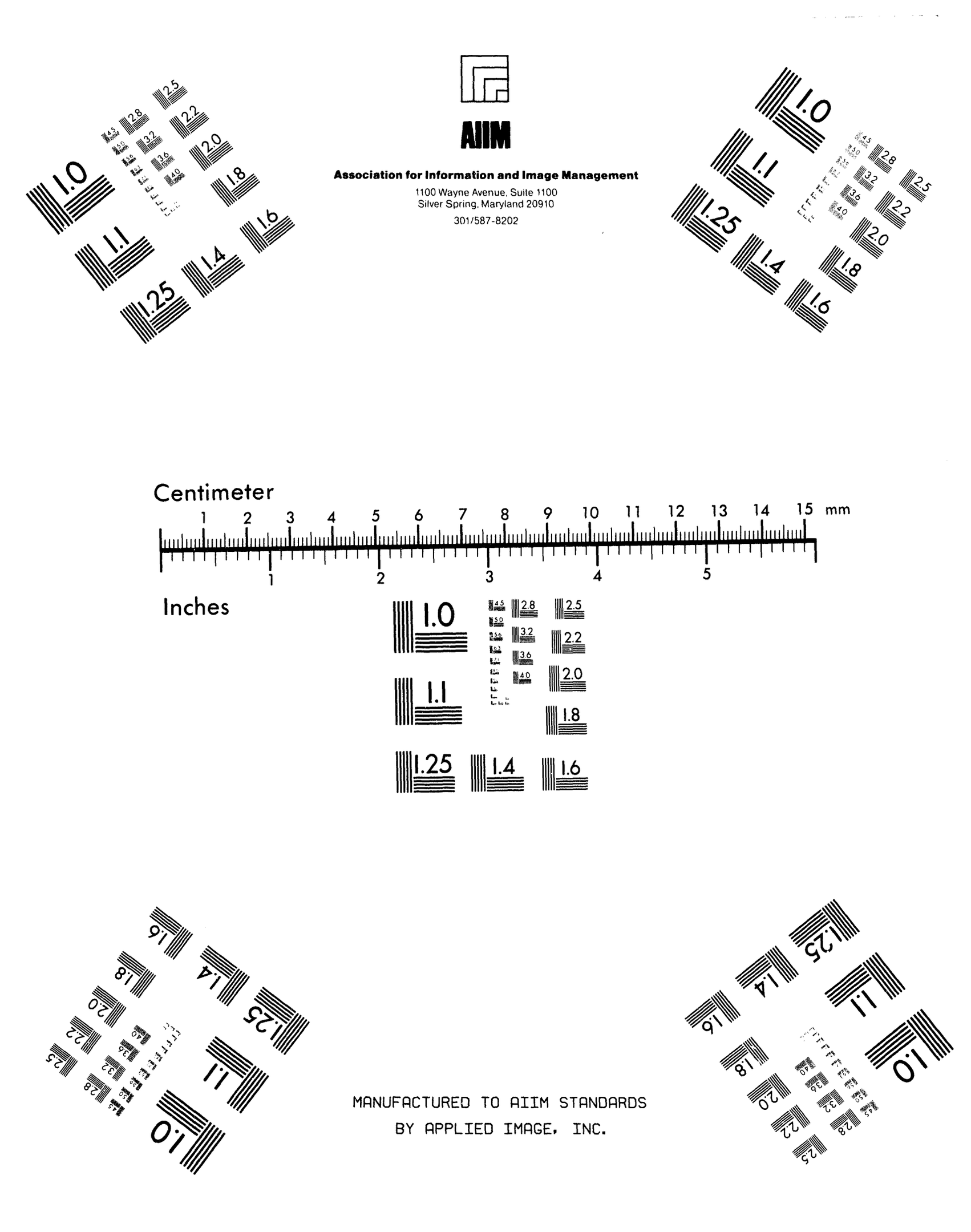
AIIM
Association for Information and Image Management
1100 Wayne Avenue, Suite 1100
Silver Spring, Maryland 20910
301/587-8202
Centimeter
Inches
MANUFACTURED TO AIIM STANDARDS
BY APPLIED IMAGE, INC.

4 of 4

sampling times for most of the flue gas trains in order to increase the sample volume and thereby reduce the detection limits for the analytes. Solid and liquid grab samples were typically collected five times per day and then combined to yield daily composites for analyses. We sampled for a total of six days over a nine-day period to collect all of the required samples.

The following list shows the analytes and the methods we used to collect flue gas samples:

Constituent	Method	Traverse/ Single Point	Duration minutes		
			In	Out	Stack
Semi-volatile organics & PCDDs/PCDFs	MM5/SW846-0010	T	216	224	360
Volatile organics	VOST	S	10,20,40	10,20,40	10,20,40
Aldehydes	Impingers	S	~45	~45	~45
Ammonia and Cyanide	Impingers	S	~45	~45	~45
Simulated plume	SRI diluter	T	-	-	360
Particle concentration	M17	T	72	-	
Gas flows	M2	T	✓	✓	✓
Metals	M29	T	196	168	360
Mercury	Carbon trap	S	50	50	50
Acid gases & Radionuclides	M5	T	96	112	360
Particle size distribution	Impactor/cyclone	T[a]	60	40	1850
Size fractionated composition	Dual cyclones	T[b]	-	-	2760
Bulk gas composition	Orsat	T[c]	✓	✓	✓

Notes: a. U of W Mk V Impactor at the stack, 5 Series Cyclone at the SDA inlet and outlet.
b. Stack only. Samples from 5 Series Cyclone train for particle size measurement used for the other size-fractionated samples for trace metals analysis.
c. Integrated sample taken in conjunction with M5 type sampling.

ANALYTICAL RESULTS

Trace Metals

Sixteen trace metals (Sb, As, Ba, Be, B, Cd, Cr, Co, Cu, Pb, Hg, Mn, Mo, Ni, Se, V) and five major metals (Al, Ca, Fe, Mg, Ti) were determined in a variety of samples. The trace metals and the corresponding sample preparation and analysis methods are listed in Table 1.

Although the 16 metals of main concern in this project are referred to as trace metals, their concentrations in the two main feed materials to the plant varied widely. In the raw coal supplied to the bunkers, barium was the most concentrated trace metal, at a concentration of about 300 µg/g; mercury was present at the lowest concentration, approximately 0.04 µg/g or a value five orders of magnitude lower. In the lime, boron and manganese were the most concentrated, at concentrations of about 100 µg/g, whereas mercury was present at the lowest level, below 0.005 µg/g.

Boron and mercury were present as vapors at high relative concentrations. Finding these metals in the vapor state was in accord with the known high vapor pressures of boron in the form of boric acid, H_3BO_3, and mercury in the forms of both the unoxidized element and the

chloride of the divalent element, $HgCl_2$. In other studies, selenium has been found to occur significantly in the vapor state; this seemed not to be the case in this investigation.

In the three ranges of particle size investigated -- roughly >8 μm, 4-8 μm, and <4 μm, the concentration of nearly every one of the trace metals increased, particularly in the step from the intermediate size range to the smallest particle size range.

Efficiencies of trace metal removal by the baghouse alone and by the combination of the spray dryer and the baghouse are presented in Table 1. The efficiency data are based on comparisons of metal concentrations at the stack with those immediately ahead of the baghouse or ahead of the spray dryer. The efficiency of the baghouse alone is the higher value, of course, because the lime and recycled solids put into the spray dryer causes an enormous elevation of the concentration of solids going into the baghouse over that going into the spray dryer. The baghouse efficiency is below 99% only for the two metals that occur significantly as vapors (boron and mercury); it exceeds 99.9% for 11 of the remaining 14 metals as the result of the extremely high efficiency of the baghouse for removing solid particles.

Other Inorganic Substances

The coal contained the non-metallic elements fluorine, chlorine, and sulfur at levels capable of producing the acidic gases HF, HCl, and SO_2 at concentrations of approximately 10, 40, and 700 ppmv, respectively. These gases were captured in an alkaline solution or peroxide, and the associated concentrations of fluoride, chloride, and sulfate ions were determined.

The amount of sulfate recovered from the gas phase was in good agreement with the expected concentration of SO_2 at the inlet to the spray dryer and was diminished about as expected, by about 60%, as the result of the acid-base reaction in the spray dryer. Fluoride and chloride were recovered at levels far below those equivalent to the expected HF and HCl concentrations. Deficiencies of fluoride and chloride in the gas phase were not compensated for with findings in the solids. The fate of the HF and HCl was thus not determined successfully; the assumption is that analytical problems of an unknown source interfered with their determination. Presumably, they were present in the flue gas, at least ahead of the spray dryer, and were removed to a significant degree by the spray dryer.

Ammonia and hydrogen cyanide were measured as minor components of the flue gas as presumed contributions from the incomplete oxidation of fuel nitrogen. Their concentrations were below 1 ppmv.

Organic Compounds

Aldehydes. These compounds were determined in various water streams and in the flue gas. Quantitation was based on the formation of stable reaction products with 2,4-dinitrophenylhydrazine (DNPH) and the measurement of each reaction product by High Performance Liquid Chromatography. The reliability of all the results on aldehydes is in doubt. One reason was the lack of success in clean-up of the DNPH reagent. The concentrations in

both water streams and in the flue gas varied widely; also, certain aldehyde compounds appeared erratically and, thus, their association with the source materials sampled is in doubt. The member of the family of compounds with the most simple structure is formaldehyde; this compound was found at apparent concentrations in water streams ranging from 40 to 300 µg/L and in flue gas at concentrations ranging from 2 to 15 µg/Nm^3. The highest concentration listed for formaldehyde was at the SDA outlet; 15 µg/Nm^3 was found as the average at the SDA outlet and 2-3 µg/Nm^3 was found as the average at the SDA inlet or the stack.

Volatile hydrocarbons. In June, 1993 SRI measured concentrations of benzene of >100 µg/Nm^3 at two locations at Springerville (spray dryer absorber (SDA) inlet and stack), and near zero concentrations at the SDA outlet. This absence of a material balance across the plant was accompanied by large variations in results at the two locations with high concentrations. We identified a potential source of contaminant in these results and returned in February, 1994 to obtain results for the volatile organic compounds (and benzene specifically) that would confirm or replace our original results. We used the normal VOST and associated sampling method with special provisions to eliminate contamination from tape on the sampling probe.

The measured benzene concentrations ranged from about 1 to 17 µg/Nm^3. Despite the scatter in these results, the range of the concentrations was in the magnitude expected. Toluene and m-,p-xylene concentrations ranged from 0 to 2 µg/Nm^3.

Semi-volatile organic compounds. These compounds were collected along with dioxins and furans in the Modified Method 5 train. The samples collected were divided during work-up, prior to compound identification, between 1) compounds commonly referred to as semi-volatiles (which include the important toxic PAH compounds) and 2) the even more toxic dioxins and furans. The first group of compounds were analyzed by low resolution GC/MS and the second group by high resolution GC/MS.

None of the group of PAHs appeared consistently in the analysis (most of the compound had minimum detectable concentrations around 0.1 µg/Nm^3). This is an important positive finding. The only identifiable compounds that appeared consistently were a small group of phthalate esters, which almost certainly were contaminants introduced inadvertently in the laboratory.

Dioxins and furans. The emphasis in the analysis was on the isomeric compounds of greatest toxicity, which have chlorine substituents at the 2, 3, 7, and 8 positions. Compounds with this feature were observed sporadically at concentrations of the order of 1 pg/Nm^3.

Material Balances

From a numerical point of view, the material balance of a metal is tested by comparing two sums, one for streams flowing into the entire system or some selected subsystem and another for streams leaving the same sphere. Each component of either sum is the product of the stream flow rate and the concentration of the metal being considered. The term "closure" is used to designate how successfully the calculated sums agree. If the sums agree exactly, the closure is 100%. If the sum for incoming streams is less than the sum for outgoing

streams, the closure is less than 100%. Conversely, if the sum for incoming streams is the larger of the two sums, the closure is larger than 100%.

There should be, ideally, a closure of 100% for stream flow rates pertinent to the entire system or each selected subsystem. For the entire system the closure of average flows was 101% and for the individual subsystems the closure of average flows ranged between 99 and 102%. The crucial data, of course, were daily concentrations of individual metals, either on a mass/mass basis (μg/g) or on a mass/volume basis (μg/Nm^3). For the major metals, the minimum closure based on average element flow rates was 85% for iron; the maximum was 129% for aluminum.

The results of tests of material balances for the 16 trace metals are shown in Figure 1. For the trace metals, the range of average closures for the overall plant lies between 36% for boron and 648% for antimony. A possible reason for the low closure for boron is that an error was made in the determination of boron in the conveyor coal. The measured boron concentration in the conveyor coal was unaccountably much lower than the boron concentration in the pulverized fuel obtained from the conveyor coal, and the closure was thus low for the pulverizer subsystem. The very high result for antimony is, in a sense, spurious, because in each subsystem, and in the overall system as well, either the input or the output (sometimes both) was indeterminate (calculations proceeded on the basis of assuming that half of the detection limit was the true value for an undetected quantity). Disregarding trace metals whose closures were influenced by non-detected quantities, the highest closure is 122% for arsenic.

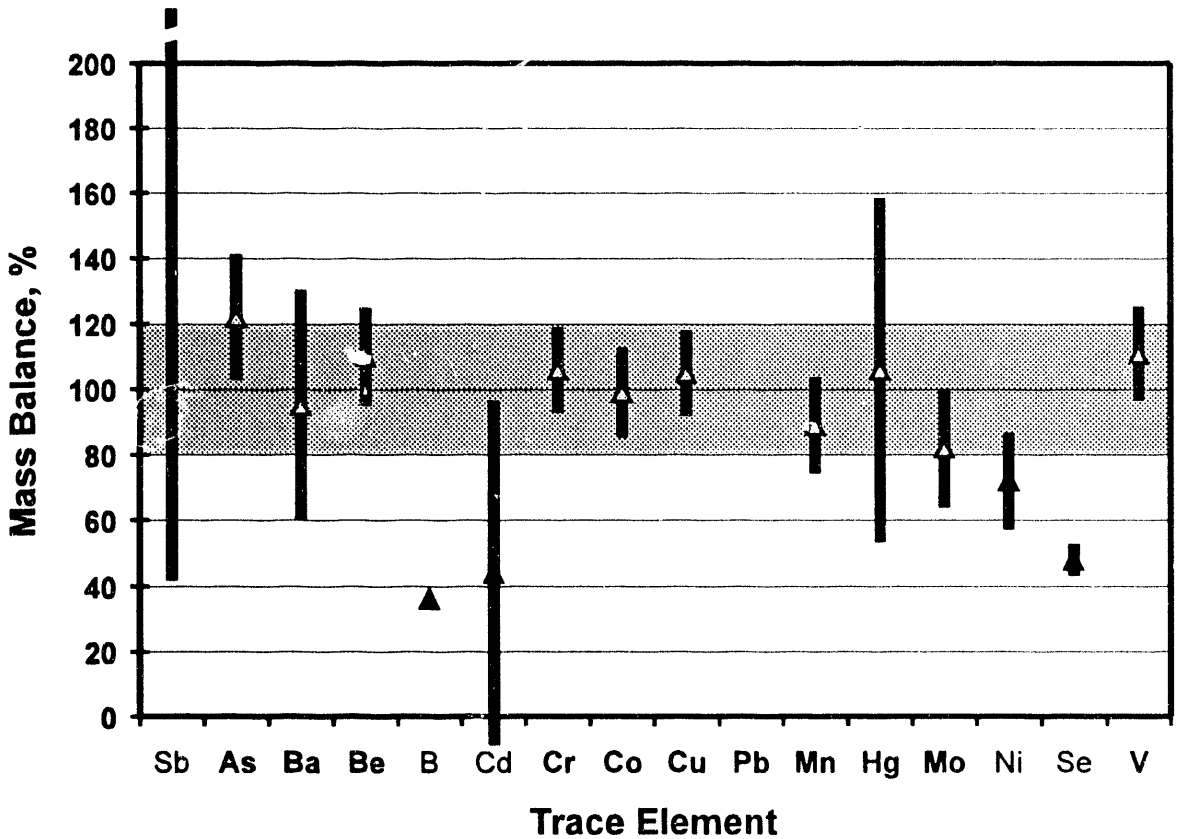

Figure 1. Overall Mass Balances of Trace Elements

Emission Factors

Emission factors are based on stack concentrations, thus reflecting whatever net control occurs in the spray dryer and the baghouse. For trace metals, the emission factors range from a value less than 0.04 lb/10^{12} Btu for beryllium to a value exceeding 600 lb/10^{12} Btu for boron. The emissions factors for the metals are presented in Table 1.

The emission factor for SO_2 is, in a relative sense, quite high — 5.2 x 10^5 lb/10^{12} Btu (sulfur, after all, is 0.7% of the fuel, and it is only controlled to the extent of 60%).

The average emissions factors for the detected organic compounds are:

Compound	Emission factor, lb/10^{12} Btu
Formaldehyde	1.4
Naphthalene	<0.12
Benzene	1.0
Toluene	0.5
m,p-Xylene	0.02
Dioxins, furans (with 2,3,7,8-chlorine substituent)	<0.000006

ACKNOWLEDGMENTS

This work was done under DOE Contract No. DE-AC22-93PC93254. Dr. Richard Tischer was replaced in December 1993 by Dr. Michael Baird of DOE/PETC as the Contracting Officer's Technical Representative for this project. Mr. Thomas Brown of DOE/PETC supervised the field sampling at Springerville. Mr. Cosimo DeMasi of Tucson Electric Power Company provided host site coordination for the test and a valuable review of the results. Mr. Joseph McCain of SRI was the sampling coordinator, Mr. John Coyne of SRI was the analytical coordinator, and Dr. Larry Monroe of SRI was the quality assurance coordinator for the work described in this manuscript.

Table 1.
TRACE METAL ANALYSES

Trace Metal	Sample Preparation [a]	Analytical Method [b]	Collection Efficiency		Emission Factors
			Across baghouse	Across overall system	lb/10^{12} Btu
Antimony	μwave digestion	HGAAS	99.7 ± 0.4	99.3 ± 1.0	0.041 ± 0.041
Arsenic	Eschka fusion	HGAAS	99.97 ± 0.05	99.9 ± 0.4	0.15 ± 0.25
Barium	μwave digestion	ICP	99.98 ± 0.01	99.95 ± 0.03	14.1 ± 4.58
Beryllium	μwave digestion	ICP	>99.98	>99.96	< 0.04
Boron	hot-plate digestion	ICP	98.0 ± 0.2	90.5 ± 5.4	609 ± 16
Cadmium	μwave digestion	GFAAS	99.995 ± 0.006	99.99 ± 0.02	0.026 ± 0.022
Chromium	μwave digestion	ICP	99.994 ± 0.004	99.99 ± 0.03	0.10 ± 0.06
Cobalt	μwave digestion	ICP	>99.96	>99.91	< 0.3
Copper	μwave digestion	ICP	99.96 ± 0.01	99.91 ± 0.06	0.98 ± 0.21
Lead	μwave digestion	GFAAS	99.7 ± 0.2	99.4 ± 0.4	0.70 ± 0.21
Manganese	μwave digestion	ICP	99.93 ± 0.01	99.80 ± 0.02	11.3 ± 4.4
Mercury [c]	open vessel	CVAAS, CVAFS	15 ± 5	25 ± 5	4.18 ± 0.69
Molybdenum	μwave digestion	ICP	99.54 ± 0.07	98.1 ± 0.6	1.4 ± 0.09
Nickel	μwave digestion	ICP	>99.97	>99.94	< 0.3
Selenium	μwave digestion	HGAAS	>99.98	>99.96	< 0.038
Vanadium	μwave digestion	ICP	99.98 ± 0.01	99.96 ± 0.02	1.0 ± 0.42

a Method for preparation of solid samples. Liquid samples were acidified with nitric acid and digested in a microwave oven.

b HGAAS - hydride generation atomic absorption spectroscopy
ICP - inductively coupled argon plasma atomic emission spectroscopy
GFAAS - graphite furnace atomic absorption spectroscopy
CVAAS - cold vapor atomic absorption spectroscopy
CVAFS - cold vapor atomic fluorescence spectroscopy

c Mercury in flue gas was sampled by Method 29 trains and iodated carbon traps: the carbon traps were analyzed by Brooks Rand, Ltd. using CVAFS.